

Chebyshev tau - QZ Algorithm Methods for Calculating Spectra of Hydrodynamic Stability Problems*

J.J. Dongarra⁽¹⁾, B. Straughan⁽²⁾ ** & D.W. Walker⁽²⁾

⁽¹⁾Department of Computer Science, University of Tennessee, Knoxville, Tennessee 37996-1301, U.S.A., and Mathematical Sciences Section, Computer Science and Mathematics Division, Oak Ridge National Laboratory, P.O. Box 2008, Oak Ridge, Tennessee 37831 - 6367, U.S.A.

⁽²⁾Mathematical Sciences Section, Computer Science and Mathematics Division, Oak Ridge National Laboratory, P.O. Box 2008, Oak Ridge, Tennessee 37831 - 6367, U.S.A.

Abstract

The Chebyshev tau method is examined in detail for a variety of eigenvalue problems arising in hydrodynamic stability studies, particularly those of Orr-Sommerfeld type. We concentrate on determining the whole of the top end of the spectrum in parameter ranges beyond those often explored. The method employing a Chebyshev representation of the fourth derivative operator, D^4 , is compared with those involving the second and first derivative operators, D^2, D , respectively. The latter two representations require use of the QZ algorithm in the resolution of the singular generalised matrix eigenvalue problem which arises. Physical problems explored are those of Poiseuille flow, Couette flow, pressure gradient driven circular pipe flow, and Couette and Poiseuille problems for two viscous, immiscible fluids, one overlying the other.

Keywords: Eigenvalue problems, Orr-Sommerfeld equations, Multi-layer flows, Chebyshev polynomials, QZ algorithm.

* This work was supported in part by the Office of Scientific Computing, U.S. Department of Energy under contract DE-AC05-84OR21400 with Lockheed Martin Energy Systems, and by the Advanced Research Projects Agency under contract DAAL03-91-C-0047, administered by the Army Research Office.

** Permanent address: Department of Mathematics, The University, Glasgow, G12 8QW, U.K.

1. Introduction

There has been much recent attention directed at solving difficult eigenvalue problems for differential equations like the Orr - Sommerfeld one, with particular interest in the removal of spurious eigenvalues or calculations in high Reynolds number ranges, cf. Abdullah & Lindsay [1], Davey [7], Fearn [13], Gardner *et al.* [14], Huang & Sloan [17], Lindsay & Ogden [18], McFadden *et al.* [19], Orszag [22], and Zebib [30]. Equations of Orr-Sommerfeld type govern the stability of shear and related flows which have important application in many fields. One such field is climate modelling with questions like determining an explanation for the origin of the mid-latitude cyclone which in turn is responsible for producing the high and low pressure regions from which variable weather patterns arise. Another application is to shear flows in electrohydrodynamic (EHD) systems which have industrial relevance in the invention of devices employing the electroviscous effect or those utilizing charge entrainment, such as EHD clutch development, or EHD high voltage generators. Yet other important mundane applications include the prediction of landslides, and flow over an aeroplane wing covered in de-icer. These topics will form part of future research.

The goal of this paper is to describe how to implement in an efficient way a Chebyshev tau - QZ algorithm method for finding eigenvalues and eigenfunctions in difficult but practical problems which occur in hydrodynamical contexts. We employ a technique which systematically writes the differential equations which occur as systems of second order equations in order to utilise the growth properties of the Chebyshev matrices which arise. One could argue that there are several other methods of finding eigenvalues/eigenfunctions and this is true. Indeed, we mention finite difference discretization coupled with a matrix technique such as the QR algorithm. We believe the method advocated here is, in general, more accurate and efficient. Other options are to employ a finite difference technique followed by inverse Rayleigh iteration, or use of compound matrices; the latter is discussed in e.g. Drazin & Reid [11], Straughan & Walker [27]. These are two viable options if one is primarily interested in only one eigenvalue. In certain hydrodynamic stability problems one may be interested in only one eigenvalue, namely the (dominant) one which is likely to contribute the most destabilizing mode in a linear instability analysis. If one can show *a priori* that a particular eigenvalue is the dominant one then a method which tracks a single eigenvalue is useful. However, for stability problems where the fluid layer is sheared it is usually not possible to show one eigenvalue is dominant. In addition, recent work has demonstrated the necessity to calculate many eigenvalues, see e.g. Butler & Farrell [3], Reddy & Henningson [23]. The Chebyshev tau - QZ algorithm method we describe finds all the eigenvalues / eigenfunctions we require in a very efficient manner. Finally, one

might wish to use a pseudospectral (collocation) technique, see e.g. Huang & Sloan [17]. Again, this is a very viable alternative. However, we believe the Chebyshev tau technique is easier to implement for problems in a cylindrical or spherical geometry where there are terms like $(m/r)d/dr$ present. Also, the growth properties of the Chebyshev tau method are likely to be better. We describe below three versions of the Chebyshev tau method which we refer to as D^4 , D^2 and D methods due to the order of the highest derivatives we discretize. It will be seen that we basically recommend the D^2 alternative because it has better growth properties than the D^4 one, whereas it makes more efficient use of the QZ algorithm than the D method which requires matrices which are twice as large.

In order to introduce some of the notation used in the fluid dynamics literature and also to describe the Chebyshev tau technique we consider a very elementary, but illuminating, example. Consider the equation and boundary conditions,

$$\begin{aligned} Lu \equiv u'' + \lambda u &= 0, & x \in (-1, 1), \\ u(-1) &= u(1) = 0, \end{aligned} \tag{1.1}$$

where the differential operator L is defined as indicated.

Now write u as a finite series of Chebyshev polynomials

$$u = \sum_{k=0}^{N+2} u_k T_k(x), \tag{1.2}$$

although the underlying logic is that (1.2) represent truncations of an infinite series. Due to the truncation, the tau method argues that rather than solving (1.1) one instead solves the equation

$$Lu = \tau_1 T_{N+1} + \tau_2 T_{N+2}, \tag{1.3}$$

where τ_1, τ_2 are tau coefficients which may be used to measure the error associated with the truncation of (1.1). In an ordinary differential equation setting as opposed to an eigenvalue background, explicit use of the tau coefficients as error bounds may be found in Fox [13].

To reduce (1.1) to a finite-dimensional problem the inner product with T_i is taken of (1.3) in the weighted $L^2(-1, 1)$ space with inner product

$$(f, g) = \int_{-1}^1 \frac{fg}{\sqrt{1-x^2}} dx,$$

and associated norm $\|\cdot\|$. The Chebyshev polynomials are orthogonal in this space, and then from (1.3) we obtain $(N + 1)$ equations

$$(Lu, T_i) = 0 \quad i = 0, 1, \dots, N. \tag{1.4}$$

There are two further conditions which arise from (1.3),

$$(Lu, T_{N+j}) = \tau_j \|T_{N+j}\|^2, \quad j = 1, 2,$$

and these may effectively be used to calculate the τ 's. The two remaining conditions are found from the boundary conditions, which since $T_n(\pm 1) = (\pm 1)^n$, yield

$$\sum_{n=0}^{N+2} (-1)^n u_n = 0, \quad \sum_{n=0}^{N+2} u_n = 0. \quad (1.5)$$

Equations (1.4) and (1.5) yield a system of $(N + 3)$ equations for the $(N + 3)$ unknowns u_i , $i = 0, \dots, N + 2$.

The derivative of a Chebyshev polynomial is a linear combination of lower order Chebyshev polynomials, in fact

$$\begin{aligned} T'_n &= 2n \sum_{k=1}^{n-1} T_k, & n \text{ even,} \\ T'_n &= 2n \sum_{k=2}^{n-1} T_k + nT_0, & n \text{ odd.} \end{aligned} \quad (1.6)$$

Then (1.4) become

$$u_i^{(2)} + \lambda u_i = 0, \quad i = 0, \dots, N, \quad (1.7)$$

where the coefficients $u_i^{(2)}$ are given by

$$u_i^{(2)} = \frac{1}{c_i} \sum_{\substack{p=N+2 \\ p=i+2 \\ p+i \text{ even}}} p(p^2 - i^2) u_p, \quad (1.8)$$

with the numbers c_i being defined by $c_0 = 2, c_i = 1, i = 1, 2, \dots$. (Actually, (1.8) is really a truncation to the $N + 2$ nd polynomial of an infinite expansion.) Equations (1.7) and (1.5) represent a matrix equation

$$A\mathbf{x} = -\lambda B\mathbf{x}, \quad (1.9)$$

with $\mathbf{x} = (u_0, \dots, u_{N+2})^T$. However, the B matrix is inevitably singular due to the way the boundary condition rows are added to A . Indeed, the last two lines of B are composed of zeros, while the upper left $(N + 1) \times (N + 1)$ part is simply the identity.

$$D^2 = \begin{pmatrix} 0 & 0 & 4 & 0 & 32 & 0 & 108 & \dots \\ 0 & 0 & 0 & 24 & 0 & 120 & 0 & \dots \\ 0 & 0 & 0 & 0 & 48 & 0 & 192 & \dots \\ \dots & \dots & \dots & \dots & \dots & \dots & \dots & \dots \end{pmatrix}$$

where we observe $D^2 = D \cdot D$ in the sense of matrix multiplication. These matrices are started at $(0, 0)$ and truncated at column $N + 2$. However, from (1.5), we easily eliminate u_{N+1}, u_{N+2} . To do this, suppose for definiteness N is odd, then

$$\begin{aligned} u_{N+1} &= -(u_0 + u_2 + \dots + u_{N-1}) \\ u_{N+2} &= -(u_1 + u_3 + \dots + u_N) \end{aligned} \quad (1.11)$$

and thus the $N + 1$ and $N + 2$ rows of D^2 may be removed and the $N + 1, N + 2$ columns eliminated using (1.11). This yields an $(N + 1) \times (N + 1)$ matrix D^2 , and the matrix problem which results from (1.9) does not suffer from B being singular due to zero boundary condition rows.

The outcome is that equation (1.1) is replaced by a system

$$A\mathbf{x} = -\lambda\mathbf{x} \quad (1.12)$$

where $\mathbf{x} = (u_0, \dots, u_N)$, and where A is now the D^2 matrix with the boundary condition rows removed as described above.

If we instead consider the solution to (1.1) by writing as a system of first order equations then we must solve

$$\begin{aligned} u' &= v, & v' &= -\lambda u, \\ u(-1) &= u(1) = 0. \end{aligned} \quad (1.13)$$

Regard u and v as independent variables and write

$$u = \sum_{k=0}^{N+1} u_k T_k(x), \quad v = \sum_{k=0}^{N+1} v_k T_k(x),$$

and then we see that solving (1.13) by a tau method requires us to solve

$$\begin{aligned} L_1(u, v) &\equiv u' - v = \tau_1 T_{N+1}, \\ L_2(u, v) &\equiv v' + \lambda u = \tau_2 T_{N+1}, \end{aligned} \quad (1.14)$$

and thus we obtain $2(N + 1)$ equations

$$\begin{aligned} (L_1(u, v), T_i) &= 0, & i &= 0, \dots, N, \\ (L_2(u, v), T_i) &= 0, & i &= 0, \dots, N, \end{aligned} \quad (1.15)$$

and two equations for the tau coefficients,

$$(L_q(u, v), T_{N+1}) = \tau_q \|T_{N+1}\|^2, \quad q = 1, 2. \quad (1.16)$$

The boundary conditions in (1.13) are again equivalent to (1.5). The finite dimensional system to be solved is then

$$u_i^{(1)} - v_i = 0, \quad v_i^{(1)} + \lambda u_i = 0, \quad i = 0, \dots, N, \quad (1.17)$$

and

$$\sum_{n=0}^{N+1} (-1)^n u_n = 0, \quad \sum_{n=0}^{N+1} u_n = 0, \quad (1.18)$$

where

$$u_i^{(1)} = \frac{2}{c_i} \sum_{\substack{p=N+1 \\ p=i+1 \\ p+i \text{ odd}}} p u_p, \quad (1.19)$$

with a similar expression for $v_i^{(1)}$.

Note that in (1.19) all the boundary conditions refer to u_i and none to v_i . Hence, we require the solution of the matrix problem

$$\begin{pmatrix} D & -I \\ BC1 & 0 \dots 0 \\ 0 & D \\ BC2 & 0 \dots 0 \end{pmatrix} \begin{pmatrix} u \\ v \end{pmatrix} = \lambda \begin{pmatrix} 0 & 0 \\ 0 \dots 0 & 0 \dots 0 \\ -I & 0 \\ 0 \dots 0 & 0 \dots 0 \end{pmatrix} \begin{pmatrix} u \\ v \end{pmatrix} \quad (1.20)$$

where $BC1, BC2$ refer to the conditions on the u_i in (1.18). We are unable to remove the boundary condition rows as before since we do not have conditions on v_i .

It is typical of the discretizations obtained in this paper that we have to solve a generalised eigenvalue problem like (1.20) and we refer to such problems in the form

$$A\mathbf{x} = \sigma B\mathbf{x}, \quad (1.21)$$

where B is, in general, singular. While the scheme leading to (1.12) yields all the eigenvalues accurately with the aid of the QZ algorithm, it is reported in Straughan & Walker [27] that (1.20) leads to the production of a spurious eigenvalue. By this we mean a number which is seen in the eigenvalue list but is not a solution to the differential equation. To elucidate on this, the QZ algorithm of Moler & Stewart [20] does not produce the eigenvalues λ_i but reduces A and B to upper triangular form with diagonal elements α_i and β_i . The eigenvalues are

$$\lambda_i = \frac{\alpha_i}{\beta_i}$$

when division makes sense. In [27] it was found that for (1.17) one value of β_i is $O(10^{-15})$ and this yields a spurious eigenvalue $O(10^{17})$. By changing N this value of λ is seen to oscillate from a very large negative value to a very large positive one and vice versa. In the fluid dynamics literature such “eigenvalues” are referred to as spurious eigenvalues and several of the references quoted deal with this topic. Indeed, McFadden *et al.* [19] write that the occurrence of spurious eigenvalues is due to rows of zero’s in B ; in this case the $N + 2$ and $2(N + 2)$ rows of B as in (1.20).

Before proceeding we should mention that the technique of writing the differential equations as systems of first order ones and discretizing is advocated by Lindsay & Ogden [18] who dealt with the Orr-Sommerfeld equation and some other equations from hydrodynamics, although they did not specifically mention the tau coefficients. Also, the idea of using (1.11) to remove boundary condition rows in the D^2 matrix was advanced by Haidvogel & Zang [15] who dealt with the solution of Poisson’s equation in a two-dimensional rectangle.

To begin our discussion of hydrodynamic stability eigenvalue problems we shall consider the Orr-Sommerfeld equation

$$(D^2 - a^2)^2 \phi = iaRe(U - c)(D^2 - a^2)\phi - iaReU''\phi, \quad z \in (-1, 1), \quad (1.22)$$

see Drazin & Reid [11], equation (25.12), where $D = d/dz$, Re , a and c are Reynolds number, wavenumber, and eigenvalue (growth rate), respectively, and ϕ is the amplitude of the stream function. For Poiseuille flow $U = 1 - z^2$, whereas for Couette flow $U = z$. Equation (1.22) is to be solved subject to the boundary conditions

$$\phi = D\phi = 0, \quad z = \pm 1. \quad (1.23)$$

In Poiseuille flow the basic flow is driven by a pressure gradient in the x -direction whereas Couette flow is driven by the upper boundary being sheared relative to the lower one. The latter is known as shear flow but the whole class of such flows is known as parallel flow.

Equation (1.22) governs the two-dimensional stability problem for parallel flow where Squire’s theorem is employed to reduce the three-dimensional problem to a two-dimensional one. This is standard knowledge in the fluid dynamics literature, cf. Drazin & Reid [11]. The function ϕ is related to the stream function ψ by

$$\psi = \phi(z)e^{ia(x-ct)}. \quad (1.24)$$

System (1.22), (1.23) has an infinite number of eigenvalues and associated eigenfunctions. Since the real part of the temporal growth rate in (1.24) is $e^{c_i t}$, $c = c_r + ic_i$, the eigenvalue which has largest imaginary part is the most dangerous in a linear instability analysis.

The component in (1.24) of the solution associated with an eigenvalue is referred to as a mode and the one with largest imaginary part is known as the dominant, or leading, mode (eigenvalue). For Poiseuille flow the first occurrence of $c_i > 0$ is when the Reynolds number is approximately 5772, see Drazin & Reid [11]. Thus, according to linearised instability theory the flow becomes unstable when $Re \geq 5772$. However, it has long been known from experimental evidence, that instabilities are seen at much lower Reynolds numbers, even around $Re = 1100$. This has led to very recent analyses which investigate the possible interaction of more than one mode, and guided by experiments, interactions of modes which pertain to a three-dimensional structure solution. Butler & Farrell [3] and Reddy & Henningson [23] are particularly interesting studies which investigate the kinetic energy associated with a finite number of modes arising in the linearised theory. For example, Butler & Farrell [3] show that modes associated with eigenvalues which have $c_i < 0$ can lead to energy growth, over a fixed time interval, of many orders of magnitude (perhaps 1000 times) greater than that associated with the leading eigenvalue. They then argue that when this happens very rapid growth is present and three-dimensional instabilities can possibly give rise to growing nonlinear terms which lead to instability at Reynolds numbers well below those of classical linear theory. The analyses of [3] and [23] are very interesting and show that one ought to consider several eigenvalues in the spectrum, not just the one with greatest imaginary part. For this reason we believe it is important to have a method which yields many eigenvalues/eigenfunctions very accurately and also in an efficient manner. The purpose of this paper is to describe such a technique, one which we refer to as the D^2 Chebyshev tau - QZ algorithm method. When we refer to the top end of the spectrum we mean those eigenvalues with c_i largest. Usually we here restrict attention to those c_i with $c_i > -1$. In analyses such as those of [3], [23] this ought to be sufficient, although lower values of c_i are easily found.

2. The Chebyshev tau methods for solving the Orr-Sommerfeld problem.

The D^4 Chebyshev tau method. Here we write, cf. Gardner *et al.* [14],

$$\phi = \sum_{i=0}^{N+4} \phi_i T_i(z), \quad (2.1)$$

in equation (1.22). Then we use the fact that

$$D^4 \phi = \sum_{i=0}^{N+4} \phi_i^{(4)} T_i(z), \quad (2.2)$$

where

$$\phi_i^{(4)} = \frac{1}{24c_i} \sum_{\substack{p=N+4 \\ p=i+4 \\ p+i \text{ even}}} p[p^2(p^2 - 4)^2 - 3p^4i^2 + 3p^2i^4 - i^2(i^2 - 4)^2] \phi_p. \quad (2.3)$$

This expression, together with expressions like (1.8) allow us to reduce (1.22) to a system of $N + 1$ equations for $\phi_0, \dots, \phi_{N+4}$, by taking the inner product with T_i . To see this define the differential operator

$$L\phi \equiv D^4\phi - 2a^2D^2\phi - ia\text{Re}(U - c)(D^2 - a^2)\phi + (a^4 - ia\text{Re}U'')\phi, \quad (2.4)$$

and then we solve exactly the equation

$$L\phi = \tau_1 T_{N+1} + \tau_2 T_{N+2} + \tau_3 T_{N+3} + \tau_4 T_{N+4}, \quad (2.5)$$

where τ_i denote tau coefficients. There should not be any confusion with our earlier use of L as it is clear from the context which operator we are referring to. We take the inner product of (2.5) with T_i for $i = 0, \dots, N$. The inner product with T_i for $i = N + 1, \dots, N + 4$ leads to four equations for the tau coefficients. The four remaining conditions are obtained from the boundary conditions (1.23), and since $T'_n(\pm 1) = (\pm 1)^{n+1}n^2$, these are

$$\sum_{i=0}^{N+4} (-1)^i \phi_i = \sum_{i=0}^{N+4} \phi_i = \sum_{i=0}^{N+4} (-1)^{i+1} i^2 \phi_i = \sum_{i=0}^{N+4} i^2 \phi_i = 0. \quad (2.6)$$

(Due to the way the terms split in the discretization of (1.22) when $U = 1 - z^2$ it is then better to write (2.6) as

$$\sum_{\substack{i=0 \\ i \text{ even}}}^{i=N+3} \phi_i = 0, \quad \sum_{\substack{i=1 \\ i \text{ odd}}}^{i=N+4} \phi_i = 0, \quad \sum_{\substack{i=1 \\ i \text{ odd}}}^{i=N+4} i^2 \phi_i = 0, \quad \sum_{\substack{i=2 \\ i \text{ even}}}^{i=N+3} i^2 \phi_i = 0. \quad (2.7)$$

In this way, one may see that the matrix problem which arises can be split into two problems, one involving ϕ_i , i odd, the other ϕ_i , i even. Then one has to solve much smaller generalised eigenvalue problems. In the general case, however, one cannot reduce the differential equation to separate even and odd mode calculations.)

Equations (2.7) can be solved to write ϕ_{N+j} $j = 1, 2, 3, 4$, as a linear combination of ϕ_0, \dots, ϕ_N . The terms ϕ_{N+j} , $j = 1, 2, 3, 4$, can then be removed in a manner not dissimilar to that for the simple example in section 1, and what results is a generalised eigenvalue problem like (1.21) with $\mathbf{x} = (\phi_0, \dots, \phi_N)$, although the matrix B which results is non-singular.

Even though B is non-singular it is important to realise that the discretization involving the fourth order derivative D^4 leads to a matrix whose terms grow like $O(M^7)$, where $M = N + 1$ is the number of polynomials. This is evident from (2.3). In actual calculations we find that a large number of polynomials are required, perhaps $M = 500$, and thus this growth rate can lead to serious round off error problems. It is worth noting that in specific calculations we use the form for D^4 given by Canuto *et al.* [4], p. 196, which rearranges (2.3) to give smaller round off error. Nevertheless, even with the Canuto *et al.* rearrangement the growth is still $O(M^7)$. Thus, we believe it is desirable to reduce the order of the differential equations whenever possible.

The D^2 Chebyshev tau method. A D^2 method writes (1.22) as two equations

$$\begin{aligned} L_1(\phi, \chi) &\equiv (D^2 - a^2)\phi - \chi = 0, \\ L_2(\phi, \chi) &\equiv (D^2 - a^2)\chi - iaRe(U - c)\chi + iaReU''\phi = 0. \end{aligned} \quad (2.8)$$

We solve exactly the equations

$$\begin{aligned} L_1(\phi, \chi) &= \tau_1 T_{N+1} + \tau_2 T_{N+2}, \\ L_2(\phi, \chi) &= \tau_3 T_{N+1} + \tau_4 T_{N+2}, \end{aligned} \quad (2.9)$$

by writing

$$\phi = \sum_{i=0}^{N+2} \phi_i T_i(z), \quad \chi = \sum_{i=0}^{N+2} \chi_i T_i(z),$$

and then by multiplying each of (2.9) in turn by T_i , $i = 0, \dots, N$. This yields $2(N + 1)$ equations for the coefficients ϕ_i, χ_i . The equations obtained by taking the inner product of (2.9) with T_{N+1}, T_{N+2} yield equations for the tau coefficients. The difficulty with the above approach, as pointed out by McFadden *et al.* [19], p. 232, is that the boundary conditions are all on ϕ_i and none are on χ_i . Thus, we cannot remove boundary condition rows by removing the $\phi_{N+1}, \phi_{N+2}, \chi_{N+1}, \chi_{N+2}$ terms which arise in the resulting D^2 matrices. (If the boundary conditions are those appropriate to surfaces free of tangential stress then there are two boundary conditions on ϕ and two on χ and one can remove the offending boundary condition rows. This we have done for Orr-Sommerfeld problems and we obtain highly accurate results and no spurious eigenvalues. Also, in a practical multi-component diffusion problem involving penetrative convection Straughan & Walker [28] arrived at similar conclusions. For porous convection problems the natural boundary conditions allow boundary condition removal in the A matrix and very satisfactory results are yielded, Straughan & Walker [26,27].)

We may instead write in the boundary conditions as rows of the matrix. This is also done by Lindsay & Ogden [18] who generalized the Gardner *et al.* [14] method and solved (1.22),

(1.23) as a system of four first order equations. We refer to their technique as a D -method and outline this below. As we have pointed out in section 1 when we use the Lindsay & Ogden [18] technique on the simple harmonic motion equation with homogeneous boundary conditions we detect a spurious eigenvalue.

A D^2 -method for (1.22), (1.23) appropriate to Poiseuille flow eventually solves an equation like (1.21) where

$$\mathbf{x} = (\phi_0, \dots, \phi_{N+2}, \chi_0, \dots, \chi_{N+2})^T,$$

with

$$A_r = \begin{pmatrix} D^2 - a^2 I & -I \\ BC1 & 0 \dots 0 \\ BC2 & 0 \dots 0 \\ 0 & D^2 - a^2 I \\ BC3 & 0 \dots 0 \\ BC4 & 0 \dots 0 \end{pmatrix}, \quad A_i = \begin{pmatrix} 0 & 0 \\ 0 \dots 0 & 0 \dots 0 \\ 0 \dots 0 & 0 \dots 0 \\ -2aReI & aRe(P - I) \\ 0 \dots 0 & 0 \dots 0 \\ 0 \dots 0 & 0 \dots 0 \end{pmatrix}$$

and

$$B_r = \mathbf{0}, \quad B_i = \begin{pmatrix} 0 & 0 \\ 0 & -aReI \\ 0 \dots 0 & \\ 0 \dots 0 & \end{pmatrix}$$

where P is the Chebyshev matrix representing z^2 , $A = A_r + iA_i$, and $B = B_r + iB_i$. (P is the matrix obtained by writing $z^2 = \frac{1}{2}(1 + T_2(z))$, and then taking the inner product $(T_i, z^2 \phi)$.)

The rows $BC1, \dots, BC4$ refer to the boundary conditions on ϕ_n and for the Orr-Sommerfeld problem we find it preferable to use the form (2.7)₁ as $BC1, BC2$ and (2.7)₂ as $BC3, BC4$.

The D Chebyshev tau method. In this case we write (1.22) as four equations

$$\begin{aligned} L_1 Y &\equiv D\phi - \zeta = 0, \\ L_2 Y &\equiv D\zeta - \eta = 0, \\ L_3 Y &\equiv D\eta - \gamma = 0, \\ L_4 Y &\equiv D\gamma - [2a^2 + iaRe(U - c)]\eta + [a^4 + ia^3 Re(U - c) + iaReU'']\phi = 0, \end{aligned} \tag{2.10}$$

where L_i denote the operators indicated and $Y = (\phi, \alpha, \beta, \gamma)$. Then write

$$\phi = \sum_{i=0}^{N+1} \phi_i T_i(z), \quad \zeta = \sum_{i=0}^{N+1} \zeta_i T_i(z), \quad \eta = \sum_{i=0}^{N+1} \eta_i T_i(z), \quad \gamma = \sum_{i=0}^{N+1} \gamma_i T_i(z). \tag{2.11}$$

Now solve exactly the tau system

$$L_m Y = \tau_m T_{N+1}, \quad m = 1, \dots, 4, \quad (2.12)$$

by multiplying each equation by T_i . This yields

$$(L_m Y, T_i) = 0, \quad m = 1, \dots, 4, \quad i = 0, \dots, N, \quad (2.13)$$

and the tau coefficients may be determined from

$$(L_m Y, T_{N+1}) = \tau_m \|T_{N+1}\|^2. \quad (2.14)$$

Equations (2.13) give $4(N+1)$ equations for the coefficients $(\phi_0, \dots, \phi_{N+1})$, $(\zeta_0, \dots, \zeta_{N+1})$, $(\eta_0, \dots, \eta_{N+1})$, $(\gamma_0, \dots, \gamma_{N+1})$. Here, a similar problem arises with the boundary conditions as with the D^2 method. The boundary conditions (2.7) involve two conditions on each of ϕ_i, ζ_i , but none on η_i, γ_i , although they are somewhat simpler being

$$\sum_{\substack{i=0 \\ i \text{ even}}}^{i=N} \phi_i = 0, \quad \sum_{\substack{i=1 \\ i \text{ odd}}}^{i=N+1} \phi_i = 0, \quad \sum_{\substack{i=0 \\ i \text{ even}}}^{i=N} \zeta_i = 0, \quad \sum_{\substack{i=1 \\ i \text{ odd}}}^{i=N+1} \zeta_i = 0. \quad (2.15)$$

The matrix problem thus becomes (1.21) with

$$A_r = \begin{pmatrix} D & -I & 0 & 0 \\ BC1 & 0 \dots 0 & 0 \dots 0 & 0 \dots 0 \\ 0 & D & -I & 0 \\ BC2 & 0 \dots 0 & 0 \dots 0 & 0 \dots 0 \\ 0 & 0 & D & -I \\ 0 \dots 0 & BC3 & 0 \dots 0 & 0 \dots 0 \\ a^4 I & 0 & -2a^2 I & D \\ 0 \dots 0 & BC4 & 0 \dots 0 & 0 \dots 0 \end{pmatrix}$$

$$A_i = \begin{pmatrix} 0 & 0 & 0 & 0 \\ 0 \dots 0 & 0 \dots 0 & 0 \dots 0 & 0 \dots 0 \\ 0 & 0 & 0 & 0 \\ 0 \dots 0 & 0 \dots 0 & 0 \dots 0 & 0 \dots 0 \\ 0 & 0 & 0 & 0 \\ 0 \dots 0 & 0 \dots 0 & 0 \dots 0 & 0 \dots 0 \\ a^3 ReU + a ReU'' & 0 & a ReU & 0 \\ 0 \dots 0 & 0 \dots 0 & 0 \dots 0 & 0 \dots 0 \end{pmatrix}$$

$$B_i = \begin{pmatrix} 0 & 0 & 0 & 0 \\ 0 \dots 0 & 0 \dots 0 & 0 \dots 0 & 0 \dots 0 \\ 0 & 0 & 0 & 0 \\ 0 \dots 0 & 0 \dots 0 & 0 \dots 0 & 0 \dots 0 \\ 0 & 0 & 0 & 0 \\ 0 \dots 0 & 0 \dots 0 & 0 \dots 0 & 0 \dots 0 \\ a^3 ReI & 0 & -aReI & 0 \\ 0 \dots 0 & 0 \dots 0 & 0 \dots 0 & 0 \dots 0 \end{pmatrix}$$

with

$$B_r = \mathbf{0}$$

where in this case $BC1 - BC4$ are $(2.15)_1 - (2.15)_4$. The vector \mathbf{x} is now

$$\mathbf{x} = (\phi_0, \dots, \phi_{N+1}, \zeta_0, \dots, \zeta_{N+1}, \eta_0, \dots, \eta_{N+1}, \gamma_0, \dots, \gamma_{N+1})^T.$$

It should be observed that in each of the D^2 and D methods the B matrices involve rows of zero's in addition to zero blocks. This is due to the way the boundary condition rows are added to A . Further, from (2.3), (1.8), and (1.19), the growth of the matrix coefficients for each of the D^4 , D^2 , and D methods is $O(M^7)$, $O(M^3)$ and $O(M)$. Finally, the D^4 , D^2 , and D methods essentially give generalised eigenvalue problems which involve A, B of order $M \times M$, $2M \times 2M$, and $4M \times 4M$.

The recent papers of Gardner *et al.* [14] and McFadden *et al.* [19] are very relevant to the present contribution and a brief discussion is in order. Gardner *et al.* [14] reduce a fourth order system to two second order ones, or, in general, reduce systems of fourth order equations to systems of second order ones. While in fluid dynamics one is often faced with an even order system, the system is not necessarily one composed of a system of fourth order equations. Gardner *et al.* [14] illustrate their method by application to the equation

$$\frac{d^4 u}{dx^4} + R \frac{d^3 u}{dx^3} - s \frac{d^2 u}{dx^2} = 0, \quad x \in (-1, 1),$$

in which R is a constant and s is the eigenvalue. The boundary conditions they take are

$$u = 0, \quad x = \pm 1; \quad u' = 0, \quad x = \pm 1.$$

To solve this they write as a second order system

$$v'' + Rv' - sv = 0, \quad u'' = v, \quad (2.16)$$

and use a tau method with

$$u(x) = \sum_{i=0}^{N+2} u_i T_i(x), \quad v(x) = \sum_{i=0}^{N+2} v_i T_i(x).$$

By multiplying (2.16) by T_i they derive $2(N+1)$ equations for the u_i, v_i and four equations for the tau coefficients. The boundary conditions yield a further four equations for the coefficients u_i, v_i .

The procedure of [14] is to eliminate the v_i coefficients since the boundary conditions are all on u_i . To do this they partition the resulting finite dimensional system as

$$\begin{aligned} B_1 \mathbf{b} + B_4 \mathbf{y} - s \mathbf{b}_1 &= \mathbf{0}, \\ B_2 \mathbf{b} + B_5 \mathbf{y} - s \mathbf{b}_2 &= \mathbf{0}, \\ \mathbf{T} &= B_3 \mathbf{b} + B_6 \mathbf{y} - s \mathbf{y}, \\ \mathbf{b} &= Q \mathbf{a}, \end{aligned} \tag{2.17}$$

where the matrices B_1, \dots, B_6 and Q are defined in [14] and where the vectors are defined by

$$\begin{aligned} \mathbf{b} &= (b_0, \dots, b_N)^T, \quad \mathbf{b}_1 = (b_0, \dots, b_{N-2})^T = Q_1 \mathbf{a}, \\ \mathbf{b}_2 &= (b_{N-1}, b_N)^T = Q_2 \mathbf{a}, \\ \mathbf{y} &= (b_{N+1}, b_{N+2})^T, \quad \mathbf{T} = (\tau_1, \tau_2)^T, \quad \mathbf{a} = (a_0, \dots, a_{N+2})^T. \end{aligned}$$

In [14] they first solve for \mathbf{y} and then reduce (2.17) to a single equation in \mathbf{a} , namely

$$(B_1 Q - B_4 B_5^{-1} B_2 Q) \mathbf{a} = s(Q_1 - B_4 B_5^{-1} Q_2) \mathbf{a}. \tag{2.18}$$

This is of form (1.21) and may be solved by the QZ algorithm. This method is extended in [14] to the Orr-Sommerfeld problem. Although the boundary condition rows may effectively be removed in this manner the problem of growth of matrix coefficients is still present. This is due to the matrices in (2.18) (equation (3.9b) of [14]). The matrices B_1 and Q each involve $\chi_2 F_2$ (in the notation of [14]) and this term is like $O(M^3)$, thus the product grows at least as $O(M^6)$ and hence the modified tau method of [14] still does not remove the growth problem. Also, it is not so evident how one would extend the Gardner *et al.* [14] method to more complicated systems such as the Butler & Farrell [3] one in three-dimensions, or the two fluid system studied in section 6 of this article.

McFadden *et al.* [19] discuss the fourth order and second order Chebyshev tau methods, paying particular attention to the differential equation system

$$\begin{aligned} \frac{d^4 u}{dx^4} &= \sigma \frac{d^2 u}{dx^2}, \quad x \in (-1, 1), \\ u(\pm 1) &= u_x(\pm 1) = 0. \end{aligned}$$

They suggest a modified tau method by discretizing (2.19) as it stands to obtain an equation of type

$$u_i^{(4)} = \sigma u_i^{(2)} \quad (2.20)$$

together with boundary conditions of type (2.6). They write equation (2.20) plus boundary conditions in the form (1.21) and then suggest setting the last two columns of the B matrix equal to zero in order to remove spurious eigenvalues. They then include an elegant proof to show that this approach is in some ways equivalent to a D^2 method which they call a stream - function vorticity method. Of course, the formulations cannot be entirely equivalent due to the growth of coefficients in the respective matrices. McFadden *et al.* [19] also discuss the Orr-Sommerfeld problem for Poiseuille flow.

In the two-dimensional case for the Orr-Sommerfeld equation the D^2 method is essentially the stream function - vorticity technique discussed by McFadden *et al.* [19]. For, in that case, the vorticity has only one component, in the y -direction, $\omega = \omega_2$ with

$$\begin{aligned} \omega &= u_{,z} - w_{,x} \\ &= \psi_{,zz} + \psi_{,xx} \\ &= e^{ia(x-ct)}(D^2 - a^2)\phi. \end{aligned}$$

Thus the functions ϕ and χ are essentially ψ and ω .

We believe that the D^2 method is more general than the stream function - vorticity method. For example, the Butler & Farrell [3] problem for Poiseuille and Couette flow in three dimensions results in a coupled system involving a fourth order equation for w and a second order equation for the normal vorticity $\omega_3 = v_{,x} - u_{,y}$. In this three-dimensional situation one may still reduce things to three second order equations and use a D^2 method which is then not equivalent to the usual stream function - vorticity method. Other areas where the D^2 method differs are in three-dimensional convection studies in anisotropic porous media where the principal axes of the permeability tensor are not orthogonal to the layer, or the Hadley flow problem, see Straughan & Walker [26,28], respectively. Although we do not include explicit details of analysis for problems such as that of Butler & Farrell [3] we stress that the extension to such three-dimensional studies is very important. Details of such studies together with the consequences for the relevant fluid mechanics may be found in a porous media setting in [26,28], although the treatment of boundary conditions is different for porous media flow.

In the remainder of the paper we make a systematic study of Chebyshev tau methods applied to Poiseuille flow, Couette flow, Hagen-Poiseuille flow, and finally we show how to apply the method to the situation where one fluid is overlying another. We stress

that we concentrate on finding many eigenvalues, including eigenvalues which are difficult to obtain, and we investigate parameter ranges which have previously proved difficult. Consideration is given to loss of accuracy due to the various D^4 , D^2 or D methods, and to loss of accuracy due to insufficient polynomials, or insufficient resolution due to lack of precision in the representation of real numbers.

3. The eigenvalue problem for plane Poiseuille flow

In this section we study (1.22), (1.23) with $U = 1 - z^2$. There have been many calculations of the spectral behaviour for Re not too large, say $Re \leq 10^4$, see Butler & Farrell [3], Drazin & Reid [11], Orszag [22], Reddy & Henningson [23], and the references therein. Abdullah & Lindsay [1], Davey [7] and Fearn [12] report studies on particular eigenvalues for Re extending to 10^9 . We use the D^2 (stream function - vorticity) method and show what can go wrong in calculating the spectrum for large Re and how one can put things right.

We have written our own codes for the D^4 , D^2 and D methods, and a comparison of results for these methods is now given.

Undoubtedly the advantage of the D^2 method is the growth rate removal, and in this respect the D method is even better, with terms growing only like $O(M)$; this important feature does not appear to have been realised in Lindsay & Ogden [18]. Against this, the time taken by the QZ algorithm appears to scale like $O(M_{\text{size}}^3)$ where M_{size} is the matrix width, i.e. $M_{\text{size}} = M, 2M, 4M$, with the D^4, D^2, D methods, respectively. The problems associated with doubling the matrix size have been commented on by McFadden *et al.* [19]. For example, on a SUN sparc station (ipc), with 50 polynomials, the D^4, D^2, D methods take, respectively, 4.1 seconds, 17.1 seconds, and 112.3 seconds. One test of the D method with $M = 150$ took 2940.7 seconds, i.e. approximately 49 minutes. Clearly, when many computations are required this is an important factor. Additionally, the memory requirements of the D method are substantial, requiring approximately 16MB for the 150 polynomial case (using full precision). The D^2 method we have found to yield high accuracy, although as reported below, for Re high enough extended precision arithmetic is required. Unless explicitly stated, our calculations are based on full precision, i.e. 64 bit, arithmetic.

The D^2 and D methods necessarily produce a B matrix in (1.21) which has one or more rows of blocks of 0's and so is singular. One approach to solving this problem is the QZ algorithm of Moler & Stewart [20]. This algorithm relies on the fact that there

exist unitary matrices Q and Z such that QAZ and QBZ are both upper triangular. The algorithm then yields sets of values α_i, β_i which are the diagonal elements of QAZ and QBZ . The eigenvalues σ_i of (1.21) are then obtained from the relation $\sigma_i = \alpha_i/\beta_i$, provided $\beta_i \neq 0$. This is very important, since the way we have constructed B means it contains a singular band, corresponding to infinite eigenvalues, and the $\beta_i = 0$ must be filtered out. Indeed, with the technique advocated here one ought always to consider the α_i and β_i , since as Moler & Stewart [20] point out, the α_i and β_i contain more information than the eigenvalues themselves. The QZ algorithm is available in the routines ZGGHRD, ZHGEQZ and ZTGEVC of the LAPACK Fortran Subroutine library, Anderson *et al.* [2]. The coefficients of the eigenvector \mathbf{x} yielded by the QZ algorithm are extremely useful convergence indicators. In this regard we throughout render the eigenvector unique by normalising so that the sum of squares of the moduli of the components is equal to one and the component of largest modulus is real. In fact, the eigenvectors can be used to indicate the presence of spurious eigenvalues. We have found by computation that the ‘‘eigenvector’’ for such a spurious eigenvalue typically does not demonstrate the convergence evident in the eigenvector for a real eigenvalue. An alternative way is to compute the τ - coefficients, cf. Gardner *et al.* [14], but as these are based on the eigenvector we find it simpler to just examine the eigenvectors themselves.

Another possible method of assessing whether an eigenvector is spurious is to compute the residuals for (1.21), i.e. compute

$$\mathbf{r}^{(i)} = \beta_i A \mathbf{x}^{(i)} - \alpha_i B \mathbf{x}^{(i)}.$$

When an ‘‘eigenvalue’’ is spurious we have found these to have *all* components between $O(10^{22})$ and $O(10^{18})$. For a real eigenvalue, the residuals corresponding to those $\beta_i = 0$ are $O(10^{18})$ as are two or three corresponding to the presence of spurious eigenvalues, whereas the rest converge from $O(10^6)$ down to $O(10^{-8})$, which is consistent with the fact that the discretization only allows us to see the ‘‘top end’’ of the true spectrum. Even though we are using a D^2 method we do find a spurious eigenvalue may be produced. When we apply the method to the problem of two fluids in section 6 then we always see spurious eigenvalues. In connection with this, we have calculated the sensitivities for the eigenvector, cf. Stewart & Sun [25], and these indicate that the spurious eigenvalues are connected with the discretization procedure rather than the QZ algorithm used to find the matrix eigenvalues. Details appropriate to the superposed fluid problem are given in section 7. A referee has kindly pointed out that relying on the eigenvector or the residuals assumes the forward stability of the QZ algorithm which cannot be assumed. However, we

have found numerically that these are reliable guides and our computations agree with, or are better than, numerical results reported by other workers.

Orszag [22] gives for $Re = 10^4$ and $a = 1$,

$$c = 0.23752649 + 0.00373967i \quad (3.1)$$

as the exact value of the first eigenvalue (to 8 d.p.). He used 56 polynomials to achieve this accuracy (although he only uses even ones, thereby only 28 terms are in his expansion). The D^4 method gives

$$c = 0.23752708 + 0.00373980i$$

with $M = 50$. We found this to be the best approximation and thereafter on increasing M the value diverges from (3.1). The D^2 and D methods, however, agree with (3.1) for $M = 56$ and beyond. We can also find the eigenfunctions very accurately. For example, the D^2 method with 56 polynomials yields ϕ_r and ϕ_i as in figure 4.20 of Drazin & Reid [11]. With the boundary conditions (2.7) or (2.15), respectively, by using the D^2 and D methods we obtained only even modes for cases when the eigenfunction is symmetric and odd modes in the skew symmetric case, and the convergence is better than that for the D^4 technique. Another feature of the D^4 method is that even though the boundary conditions are removed we still saw two values in the list with $\beta = 0$. The corresponding α values were large, $O(10^{15})$, and real. These we believe are spurious but are easily filtered out by examining the β_i given by the QZ algorithm. This does raise an important point. It questions whether the only way spurious eigenvalues can arise is through rows of zero's in the B matrix due to inserting boundary condition rows in the equivalent row(s) of A .

Orszag [22] table 5 gives a list of the 32 least stable modes for $Re = 10^4$, $a = 1$. With the D^2 method we obtained complete agreement with this list in the sense: for the first 12 eigenvalues with 70 polynomials, for the first 14 eigenvalues with 80 polynomials, and complete agreement with all 32 eigenvalues by using 96 polynomials. We did, however, find an extra eigenvalue; between positions 17 and 18 of Orszag [22] table 5 we obtain the value

$$c = 0.21272578 - 0.19936069i. \quad (3.2)$$

The eigenvector coefficients from the D^2 method (normalised as indicated earlier) with 96 polynomials indicate the value (3.2) corresponds to a skew-symmetric solution and with this number of polynomials the eigenvector had converged to $O(10^{-13})$, $O(10^{-14})$, for the ϕ and A ($= D^2\phi - a^2\phi$) terms. Interestingly, we find both symmetric and skew symmetric modes with the D (and D^2) method(s). Lindsay & Ogden [18] appear to report only symmetric ones. For $Re = 10^4$, $a = 1$, the spectrum, in the range $c_i \in (-1, 0)$, $c_r \in (0, 1)$,

is given in figure 1, indicating which are even and which are odd modes. When we refer to the spectrum in a figure here and throughout the paper we mean that part displayed in the relevant figure.

We have produced an mpeg movie which may be accessed with a web browser, such as Mosaic or Netscape, at

<http://www.epm.ornl.gov/~walker/eigenproblems.html>

This movie contains the parametric evolution of the spectrum of the plane Poiseuille flow problem for $a = 1$, with Re ranging from 100 to 10^4 in steps of 10. This may yield useful insight into resonance mechanisms. The evolution of the upper branches is clearly visible and the emanence of the eigenvalues from $c_r = 2/3$ is evident.

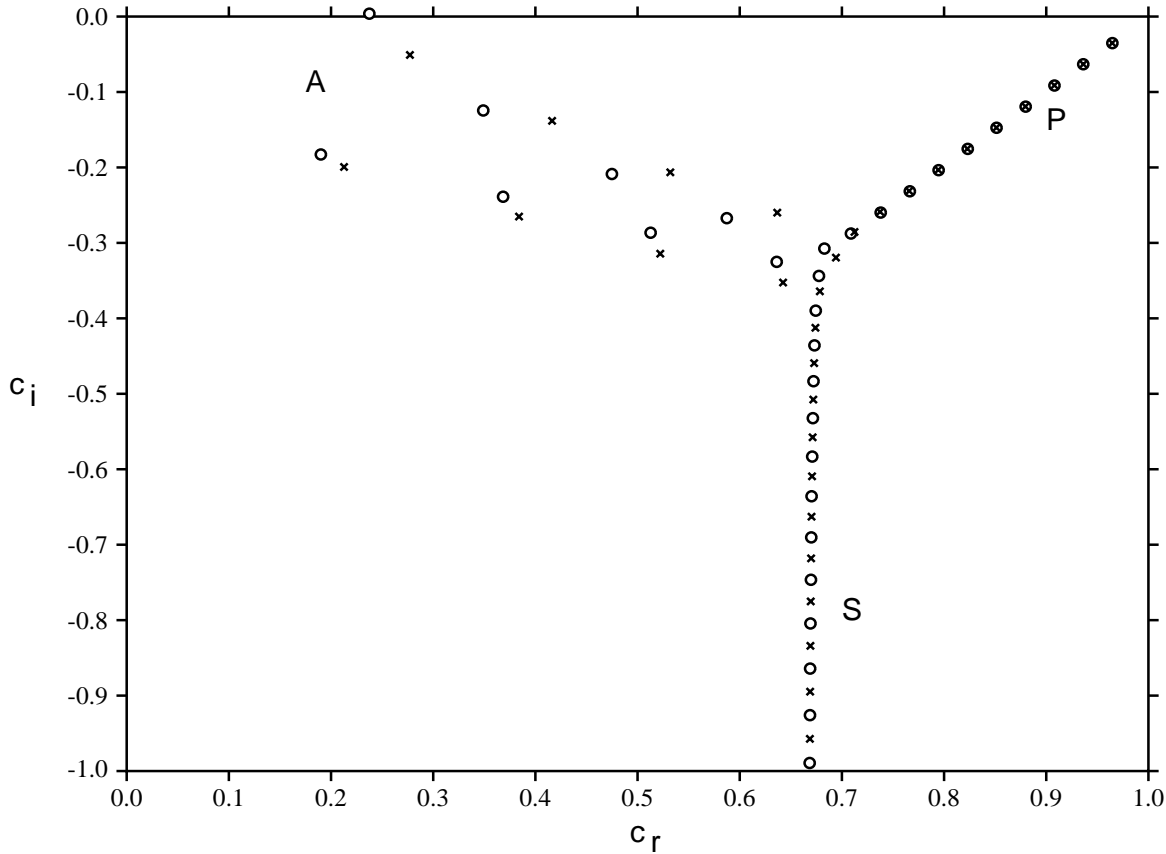


Figure 1 The spectrum for plane Poiseuille flow. $Re = 10^4$, $a = 1$, open circle (o) = even eigenfunction, cross (\times) = odd eigenfunction. The upper right branch consists of “degenerate” pairs of even and odd eigenvalues.

When Re is increased eventually mode crossing is seen, i.e. eigenvalues exchange positions in the sense that the imaginary part of one eigenvalue decreases relative to that of another eigenvalue whose imaginary part eventually becomes larger than that of the former. Abdullah & Lindsay [1] are critical of the papers of Davey [7] and Fearn [12] in their analysis of higher Re values. According to linear theory for (1.22) and (1.23) the most unstable eigenvalue has largest imaginary part, i.e. c_i largest. Davey [7] claims the most unstable mode is symmetric, presumably on the basis that this is so for $Re = 10^4$, $a = 1$. Fearn [12] solves a symmetric problem and simply refers to *the solution* to (1.22), confirming Davey’s [7] results. Abdullah & Lindsay [1] claim that these writers are using a tracking technique and miss the leading eigenvalue since mode crossing occurs. We have partially confirmed the findings of Abdullah & Lindsay [1] and Lindsay & Ogden [18] who only give the first five eigenvalues, although it would appear they find only symmetric

ones. This is especially important, since for $Re = 10^5$, $a = 1$, we confirm mode crossing has occurred, but we find the leading eigenvalue to be skew-symmetric. We present in table 1 the leading eigenvalues for $Re = 10^5$ and $a = 1$, our calculations being made by a D^2 method, but determining odd modes and even modes separately, with $M = 200$ in each case, i.e. equivalent to $M = 400$ for the full problem.

It is seen from table 1 that the “leading” eigenvalue is a skew - symmetric one. In table 2 we include components of the (normalised) eigenvector for this skew mode. It is seen that machine precision is reached with 86 odd polynomials, i.e. up to T_{171} . (All components are not included, just a sample to demonstrate convergence.)

We have used the separate “odd” and “even” codes with $M = 200$ to compute the behaviour of the eigenvalues in the transition region. For $a = 1$, in table 3 it is seen that the structure at $Re = 10^4$ is maintained at $Re = 80,822$ but by $Re = 80,828$ the first two eigenvalues exchange positions, then by $Re = 80,830$ the eigenvalue which is second at $Re = 80,828$ exchanges with the one occupying third position for the same Re value. The position of these three is maintained in table 1.

Abdullah & Lindsay [1] report further mode crossings for higher Re values. However, much care must be taken when Re increases. We now report findings for the spectrum and in particular in the region near the joining of the so called A, P and S branches - the three groups of branches in figure 1. As indicated in the figure the A branches are the upper left ones, the P branch is the upper right one composed of degenerate pairs, and the S branch is the lower one emanating from $c_r = 2/3$. This notation is standard in the fluid dynamics literature, see Drazin & Reid [11]. The eigenvalues near the branch point are particularly sensitive to change, Orszag [22], and we find great care must be taken even with Re around 2.3×10^4 .

We have computed many cases and figures 2-5 below are just a sample. Even though they are only for even modes they illustrate the important points regarding round off error. The same findings are true for odd mode cases, and for the full code which finds odd and even modes together.

Figures 2 to 5 are obtained with the D^2 method solving (1.22), (1.23) for even modes only, i.e. employing only even polynomials, using full precision arithmetic (64 bit) in figures 2 to 4, whereas extended precision (128 bit) is employed in figure 5. Figure 2 demonstrates inaccuracy caused by having insufficient polynomials, even though $M = 85$, (equivalent to 170 in the odd and even code). This splitting in the tail is symptomatic of insufficient polynomials and we find similar behaviour in all of the problems reported here. By increasing the number of polynomials we are able to overcome the splitting of the tail problem as in figure 3 where $M = 200$. Nevertheless, the eigenvalues at the intersection

are not accurate. Increasing the number of polynomials compounds the problem and we find a “triangle of numerical instability” begins to form, figure 4, where $M = 500$. We have found that this behaviour is due to the precision to which we are working. By increasing from 64 to 128 bit arithmetic this effect is removed (in this case), see figure 5. We have not seen the latter effect reported before. The 128 bit arithmetic calculations were performed with the LAPACK routines on an IBM RS 6000 590 machine.

A referee raised the very interesting question as to whether the D^2 method operating at 128 bit arithmetic is as expensive as the D method at 64 bit arithmetic. From the computational time point of view the two methods are comparable. However, we have ran the D method in 64 bit arithmetic for the cases of figures 2 to 4. The instability at the intersection of the branches is *not* removed. Thus, the D^2 method at 128 bit arithmetic is *not* equivalent to the D method at 64 bit arithmetic. The instability seen in figures 2 to 4 is not due to growth of coefficients in the A matrix and we believe that it can only be removed by increasing the precision. This, of course, raises the question of when to use a certain precision, and how many polynomials we should employ *a priori*. This point was succinctly raised by a referee. At present we do not have an analytical answer to this. We have proceeded by numerical experiment and comparison with previous work. We are investigating further this aspect and, indeed, the question of how spurious eigenvalues form. Nevertheless, we believe the findings we report here are worthy and ought to be brought to the attention of workers dealing with practical hydrodynamical stability problems.

Symmetry	Eigenvalue
A	.9888191058E + 00 - .1116257893E - 01i
A	.9798738045E + 00 - .2008374163E - 01i
A	.9709280339E + 00 - .2900433538E - 01i
A	.1373944878E + 00 - .2956356969E - 01i
A	.9619817790E + 00 - .3792441466E - 01i
A	.9530350180E + 00 - .4684401422E - 01i
S	.9888195933E + 00 - .1116360699E - 01i
S	.1459247829E + 00 - .1504203085E - 01i
S	.9798751271E + 00 - .2008635538E - 01i
S	.9709305305E + 00 - .2900898101E - 01i
S	.1982003566E + 00 - .3733100660E - 01i
S	.9619857994E + 00 - .3793148490E - 01i

Table 1. The six odd and six even eigenvalues with largest imaginary part for the Orr-Sommerfeld problem with $U = 1 - z^2$, $Re = 10^5$, $a = 1$. A=anti-symmetric, S=symmetric.

Com. No.	ϕ_r	ϕ_i	A_r	A_i
1	.208839E-03	.409542E-03	.240779E-01	.204308E-01
11	.421908E-03	.289300E-03	-.167597E+00	-.125165E+00
21	.889307E-04	-.897408E-04	-.147664E+00	.148864E+00
31	-.123273E-04	-.114027E-05	.458675E-01	.307459E-02
41	.461222E-06	.686801E-07	-.304143E-02	-.281158E-03
51	-.553081E-08	.346867E-08	.525270E-04	-.400853E-04
61	-.122030E-10	-.307889E-10	.231698E-06	.414265E-06
71	.456178E-13	-.465328E-13	-.665353E-09	.937961E-09
81	-.147851E-14	-.190889E-14	-.960477E-12	.301479E-12
86	.153318E-14	.354368E-14	-.262614E-14	.292893E-14

Table 2. A selection of the components of the eigenvector corresponding to $\sigma^{(1)} = 0.9888191058 - 0.01116257893i$, $Re = 10^5$, $a = 1$. Com. No. refers to the component of the eigenvector, $\phi = \phi_r + i\phi_i$, $A = A_r + iA_i$. The eigenvector is normalised with the sum of squares of the moduli of the components equal to one and the component of largest modulus is real.

Symmetry	Eigenvalue	Re
A	$.9875629891E + 00 - .1241421339E - 01i$	80822
A	$.9776125822E + 00 - .2233449266E - 01i$	80822
A	$.1470238117E + 00 - .3124631640E - 01i$	80822
A	$9676615245E + 00 - .3225401228E - 01i$	80822
S	$.1555554132E + 00 - .1241409956E - 01i$	80822
S	$.9875636361E + 00 - .1241555934E - 01i$	80822
S	$.9776143504E + 00 - .2233791980E - 01i$	80822
S	$.9676648840E + 00 - .3226011142E - 01i$	80822
A	$.9875634508E + 00 - .1241375347E - 01i$	80828
A	$.9776134133E + 00 - .2233366562E - 01i$	80828
A	$.1470203436E + 00 - .3124575284E - 01i$	80828
A	$.9676627251E + 00 - .3225281822E - 01i$	80828
S	$.1555521082E + 00 - .1241509695E - 01i$	80828
S	$.9875640977E + 00 - .1241509935E - 01i$	80828
S	$.9776151812E + 00 - .2233709233E - 01i$	80828
S	$.9676660845E + 00 - .3225891687E - 01i$	80828
A	$.9875636047E + 00 - .1241360017E - 01i$	80830
A	$.9776136903E + 00 - .2233338998E - 01i$	80830
A	$.1470191935E + 00 - .3124557862E - 01i$	80830
A	$.9676631252E + 00 - .3225242025E - 01i$	80830
S	$.9875642516E + 00 - .1241494596E - 01i$	80830
S	$.1555510002E + 00 - .1241538251E - 01i$	80830
S	$.9776154583E + 00 - .2233681675E - 01i$	80830
S	$.9676664843E + 00 - .3225851880E - 01i$	80830

Table 3. The four leading odd and even eigenvalues in the transition region, $M = 200$, $a = 1$.

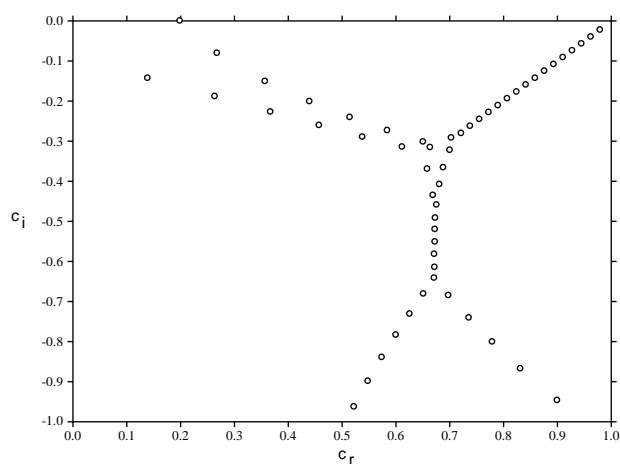


Figure 2

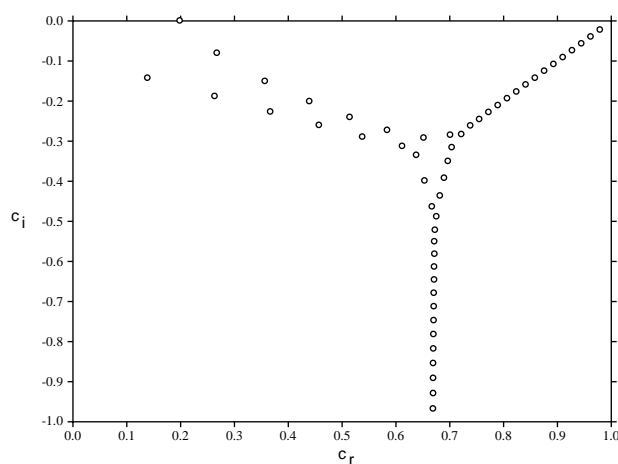


Figure 3

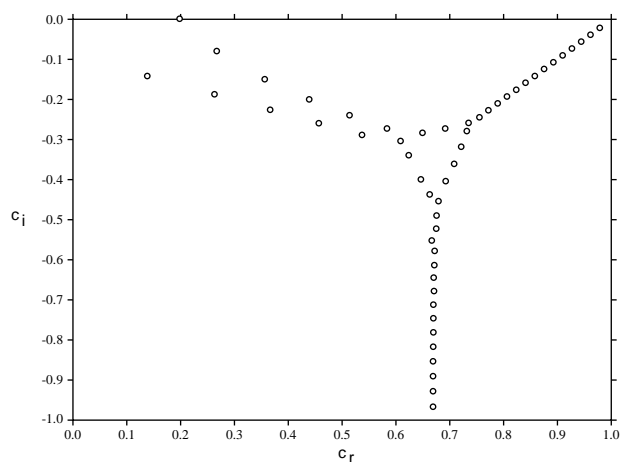


Figure 4

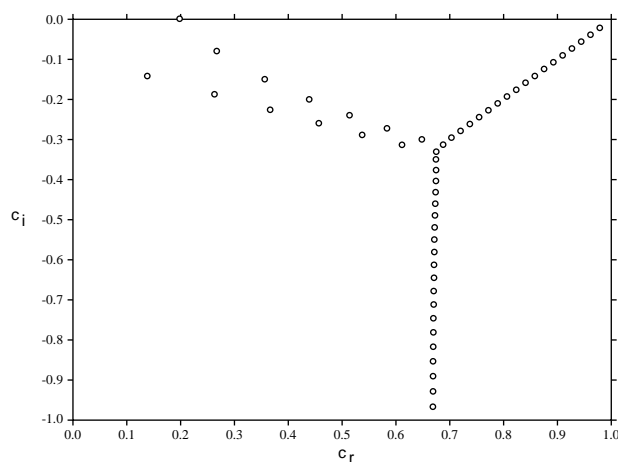


Figure 5

Figure 2 The approximate eigenvalues associated with even modes for plane Poiseuille flow. Effect of too few polynomials. $Re = 2.7 \times 10^4$, $a = 1$, $M = 85$, 64 bit arithmetic.

Figure 3 The approximate eigenvalues associated with even modes for plane Poiseuille flow. Effect of finite precision. $Re = 2.7 \times 10^4$, $a = 1$, $M = 200$, 64 bit arithmetic.

Figure 4 The approximate eigenvalues associated with even modes for plane Poiseuille flow. Effect of finite precision. $Re = 2.7 \times 10^4$, $a = 1$, $M = 500$, 64 bit arithmetic.

Figure 5 The approximate eigenvalues associated with even modes for plane Poiseuille flow. $Re = 2.7 \times 10^4$, $a = 1$, $M = 200$, 128 bit arithmetic.

Remarks. To conclude this section we note that we have drawn attention to three important types of error which are present in solving difficult eigenvalue problems. The first is round off error due to growth of matrix coefficients. In this respect a D^2 method is preferable to one using D^4 . Secondly, too few polynomials causes the “tail”, i.e. the S branch, to split. Thirdly, increasing the number of polynomials in a cavalier fashion to compute sensitive eigenvalues can lead to inaccuracy due to ill conditioning and insufficient precision in real number representation. Clearly care must be taken to avoid these errors and while our work regarding the latter two is heuristic, we believe it is worth drawing attention to these points, while we continue in a search for analytical tests to determine the correct number of polynomials coupled with the best precision.

4. The eigenvalue problem for plane Couette flow

The problem of this subsection is (1.22) and (1.23) when $U = z$. Physically it corresponds to the lower plate fixed while the upper plate is moved with constant velocity, generating a linear shear. This problem is always stable according to linear theory, cf. Drazin & Reid [11]. Nevertheless, it is not a trivial eigenvalue problem from a numerical standpoint. Indeed, we studied this problem at the suggestion of Dr. Alison Hooper who informed us she had difficulty in calculating the spectrum for Reynolds numbers as low as 2000.

With 150 polynomials in the D^2 method we obtain excellent accuracy for $Re = 3000$, $a = 1$, in 64 bit arithmetic. Breakdown at the intersection of the branch points is evident around $Re = 3500$. However, the same code operating at 128 bit arithmetic yields an accurate spectrum.

In 128 bit arithmetic we are able to extend the calculation well beyond $Re = 3800$. With 150 polynomials no difficulty is experienced at $Re = 8000$, but at $Re = 10^4$ a split in the tail is observed. By using 200 polynomials and 128 bit arithmetic we have been able to proceed to $Re = 13,000$, and the spectrum for this case is shown in figure 6. For the benefit of others who might use this calculation as a yardstick we present actual numerical values in table 4.

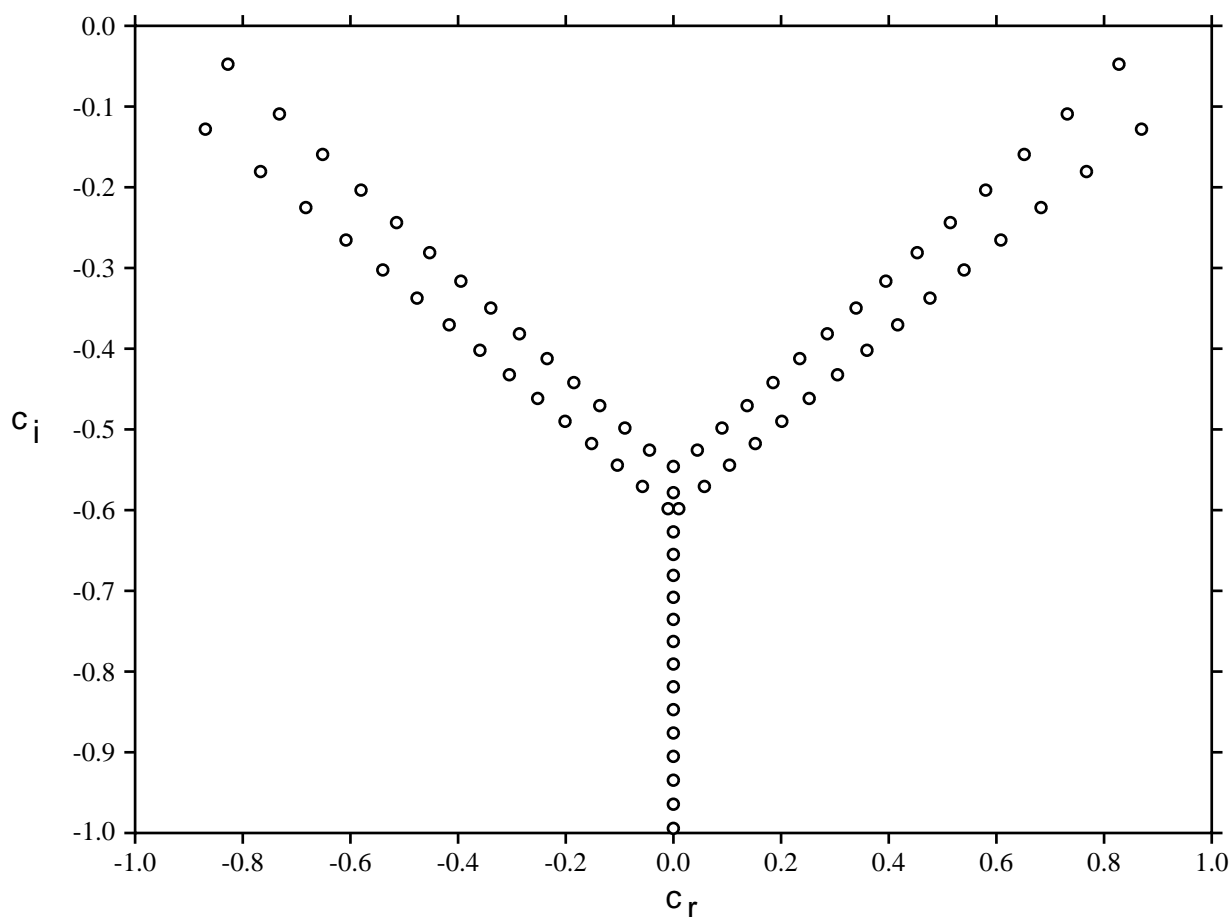


Figure 6 The spectrum for plane Couette flow, using 200 polynomials. $Re = 13,000$, $a = 1$, 128 bit arithmetic.

Mode number	Eigenvalue c
1	$\pm .8276152337E + 00 - .4751548439E - 01i$
2	$\pm .7318167785E + 00 - .1091860424E + 00i$
3	$\pm .8694486153E + 00 - .1279149536E + 00i$
4	$\pm .6516804277E + 00 - .1594003003E + 00i$
5	$\pm .7671186628E + 00 - .1805164930E + 00i$
6	$\pm .5801567166E + 00 - .2035572830E + 00i$
7	$\pm .6828371673E + 00 - .2251746419E + 00i$
8	$\pm .5143995235E + 00 - .2437675825E + 00i$
9	$\pm .6082408213E + 00 - .2653481107E + 00i$
10	$\pm .4528935800E + 00 - .2811241939E + 00i$
11	$\pm .5400219613E + 00 - .3024678732E + 00i$
12	$\pm .3947096982E + 00 - .3162828159E + 00i$
13	$\pm .4764491821E + 00 - .3373108149E + 00i$
14	$\pm .3392256967E + 00 - .3496747907E + 00i$
15	$\pm .4164746866E + 00 - .3703603829E + 00i$
16	$\pm .2859989475E + 00 - .3816025000E + 00i$
17	$\pm .3594042660E + 00 - .4019439818E + 00i$
18	$\pm .2347002407E + 00 - .4122880439E + 00i$
19	$\pm .3047483827E + 00 - .4322966352E + 00i$
20	$\pm .1850762211E + 00 - .4419004929E + 00i$
21	$\pm .2521456926E + 00 - .4615944208E + 00i$
22	$\pm .1369265577E + 00 - .4705722463E + 00i$
23	$\pm .2013199914E + 00 - .4899736516E + 00i$
24	$\pm .9008929422E - 01 - .4984093248E + 00i$
25	$\pm .1520542459E + 00 - .5175426311E + 00i$
26	$\pm .4444142747E - 01 - .5255273887E + 00i$
27	$\pm .1041741466E + 00 - .5443892453E + 00i$
28	$.0000000000E + 00 - .5459244238E + 00i$
29	$\pm .5753309952E - 01 - .5705930815E + 00i$
30	$.0000000000E + 00 - .5782633202E + 00i$
31	$\pm .9937461129E - 02 - .5982573646E + 00i$
32	$.0000000000E + 00 - .6268958614E + 00i$
33	$.0000000000E + 00 - .6550042769E + 00i$
34	$.0000000000E + 00 - .6809093456E + 00i$
35	$.0000000000E + 00 - .7081327166E + 00i$
36	$.0000000000E + 00 - .7352566431E + 00i$
37	$.0000000000E + 00 - .7628468874E + 00i$
38	$.0000000000E + 00 - .7906653030E + 00i$
39	$.0000000000E + 00 - .8188353645E + 00i$
40	$.0000000000E + 00 - .8472841070E + 00i$
41	$.0000000000E + 00 - .8760700653E + 00i$
42	$.0000000000E + 00 - .9051510243E + 00i$
43	$.0000000000E + 00 - .9345643207E + 00i$
44	$.0000000000E + 00 - .9642865284E + 00i$
45	$.0000000000E + 00 - .9943359829E + 00i$

Table 4. The first 45 eigenvalues graphed in figure 6. Conjugate pairs are presented as one mode.

5. The eigenvalue problem for circular pipe flow

Symmetric disturbances for the linear instability problem for flow in a circular pipe driven by a constant pressure gradient (Hagen - Poiseuille flow) are governed by the equation

$$L^2 \phi = iaRe(U - c)L\phi, \quad (5.1)$$

where a, Re, c are wavenumber, Reynolds number, and growth rate, respectively, the base velocity $U = 1 - r^2$, r being the radial coordinate, the differential operator L is defined by

$$L = \frac{d^2}{dr^2} - \frac{1}{r} \frac{d}{dr} - a^2, \quad (5.2)$$

and (5.1) holds on the domain $r \in (0, 1)$. The disturbance ϕ is subject to the boundary conditions

$$\phi = \phi' = 0, \quad r = 0, 1, \quad (5.3)$$

cf. Drazin & Reid [11]. Symmetric disturbances governed by (5.1)-(5.3) are believed always stable, Drazin & Reid [11].

We show how to solve (5.1)-(5.3) by a D^2 Chebyshev tau - QZ algorithm method. This avoids the growth problem associated with direct discretization of the fourth order derivative. It is worth pointing out that this technique will have wide application since there are many technologically important problems in fluid flows in a pipe, or in a pipe filled with porous material. Also, the D^2 technique is perfectly suited to hydrodynamic stability studies of flows in a spherical geometry. The singular terms of form $(m/r)d/dr$ which occur in such problems may be handled perfectly naturally using the properties of Chebyshev polynomials. The boundary value problem (5.1)-(5.3) is solved by a D^2 method by writing

$$\begin{aligned} L\phi &= \psi, \\ L\psi &= iaRe(U - c)\psi, \end{aligned} \quad (5.4)$$

subject to (5.3). Define L_1, L_2 by

$$\begin{aligned} L_1(\phi, \psi) &\equiv L\phi - \psi, \\ L_2(\phi, \psi) &\equiv L\psi - iaRe(U - c)\psi. \end{aligned} \quad (5.5)$$

To use the Chebyshev tau method on this system we transform to $z = 2r - 1$ and then use the key relation, Orszag [22],

$$T_{m+1}(z) + T_{m-1}(z) = 2zT_m(z), \quad m \geq 1. \quad (5.6)$$

In terms of z the operator L becomes

$$L \equiv 4 \frac{d^2}{dz^2} - \frac{4}{(z+1)} \frac{d}{dz} - a^2$$

and

$$U = \frac{3}{4} - \frac{1}{2}z - \frac{1}{4}z^2.$$

Then we solve exactly the tau system

$$\begin{aligned} L_1(\phi, \psi) &= \frac{\tau_1}{(z+1)} T_{N+1} + \frac{\tau_2}{(z+1)} T_{N+2}, \\ L_2(\phi, \psi) &= \frac{\tau_3}{(z+1)} T_{N+1} + \frac{\tau_4}{(z+1)} T_{N+2}. \end{aligned} \tag{5.7}$$

To remove the singularity we multiply each equation in (5.6) by $(z+1)T_m$ and integrate in the weighted $L^2(-1, 1)$ space with weight $(1-z^2)^{-1/2}$. While we now have to calculate terms like $(zT_m, \frac{d^2\phi}{dz^2})$ the beauty of using the weighted inner product is the natural removal of the singular term in L .

After some calculation we arrive at an equation of form (1.21) where

$$A_r = \begin{pmatrix} 4ZD^2 + 4D^2 - 4D - a^2(Z+I) & -(Z+I) \\ BC1 & 0 \dots 0 \\ BC2 & 0 \dots 0 \\ 0 & 4ZD^2 + 4D^2 - 4D - a^2(Z+I) \\ BC3 & 0 \dots 0 \\ BC4 & 0 \dots 0 \end{pmatrix}$$

$$A_i = \begin{pmatrix} 0 & 0 \\ 0 \dots 0 & 0 \dots 0 \\ 0 \dots 0 & 0 \dots 0 \\ 0 & aRe(\frac{1}{4}Z^3 + \frac{3}{4}Z^2 - \frac{1}{4}Z - \frac{3}{4}I) \\ 0 \dots 0 & 0 \dots 0 \\ 0 \dots 0 & 0 \dots 0 \end{pmatrix}$$

and

$$B_r = \mathbf{0}, \quad B_i = \begin{pmatrix} 0 & 0 \\ 0 & -aReI \\ & 0 \dots 0 \\ & 0 \dots 0 \end{pmatrix}$$

where

$$\mathbf{x} = (\phi_0, \dots, \phi_{N+2}, \psi_0, \dots, \psi_{N+2})^T,$$

Z^n denotes the matrix arising from the Chebyshev representation of the function z^n , ZD^2 being the Chebyshev representation of zD^2 . The boundary conditions $BC1 - BC4$ are those of (2.7).

Although we do not include numerical output for the problem of this section we have carried out many computations. The behaviour seen in sections 3 and 4 is also observed here. The spectrum has a similar shape to that seen in section 3 and too few polynomials lead to a split in the tail. Again, for high Reynolds numbers instability is witnessed at the intersection of the branch points but it may be remedied by increasing the precision.

6. The eigenvalue problem for Orr-Sommerfeld like flows for two superposed immiscible fluids.

Here we study the eigenvalue problem associated to the problem of Couette and / or Poiseuille flow when one immiscible viscous fluid overlies another. This is a problem of major technological importance with application from the oil industry to fields such as de-icing of an aeroplane wing, cf. Chen & Crighton [5]. Many references may be found in the papers by Chen & Crighton [5], Hooper [16], and Renardy [24]. While we here develop a D^2 method for the situation studied by Hooper [16] we believe the ideas are extendable to more complicated scenarios such as the one of Chen & Crighton [5]. We stress that the D^2 Chebyshev tau method has wide application to many hydrodynamic stability studies and we are presenting it here as a guide as to how one would apply it in other two or multi-layer situations. In particular, we believe it is an ideal method to apply to two or many layer fluid flows in a pipe where the singular terms may be handled as outlined in section 5. Inclusion of electric and magnetic effects greatly increases the order of the system, but the D^2 Chebyshev method is perfectly suited to incorporate such effects.

Hooper [16] assumes a fluid, denoted by 2, is overlying a different, immiscible fluid, denoted by 1, the configuration being contained in a horizontal position between planes $y = -1, y = n$, with the (x, z) -plane horizontal while the y -axis is vertical (orthogonal to the bounding planes of the fluids). The dynamic viscosities, densities and depths in each fluid are denoted by μ_α, ρ_α and d_α , respectively, $\alpha = 1, 2$. The upper plane $y = n$ may be subject to a (dimensionless) velocity in the x -direction, u_n , and the velocity of the interface (in the steady state) is U_{int} . A Reynolds number, Re , is defined with respect to U_{int} . The basic flow has form

$$\begin{aligned} u_1(y) &= A_1 y^2 + a_1 y + 1, & -1 < y < 0, \\ u_2(y) &= A_2 y^2 + a_2 y + 1, & 0 < y < n, \end{aligned} \tag{6.1}$$

where

$$\begin{aligned} A_1 &= \frac{-(m+n) + mu_n}{n(n+1)}, \\ a_1 &= \frac{n^2 - m + mu_n}{n(n+1)}, \\ A_2 &= \frac{A_1}{m}, \quad a_2 = \frac{a_1}{m}, \end{aligned} \tag{6.2}$$

with m and n being the viscosity and depth ratios,

$$m = \frac{\mu_2}{\mu_1}, \quad n = \frac{d_2}{d_1}. \tag{6.3}$$

Hooper [16] observes that $u_n = 0$ gives rise to a two fluid version of plane Poiseuille flow, whereas $u_n = (m+n)/m$ yields Couette flow. Renardy [24], pp. 1762, 1763, includes a detailed account of the applicability of Squire's theorem to two fluid flows and points out that if there are islands of stability (where the neutral curve consists of one or more isolated closed curves in addition to the usual convex one, as occurs in multi - component convection - diffusion, cf. Straughan & Walker [28]) then such a theorem would not be applicable. In that case one would be faced with a three-dimensional analysis and a D^2 method is not equivalent to a stream function - vorticity method. However, we stress that the D^2 method is still applicable in that case. We here follow Hooper [16] and analyse directly the two-dimensional situation. Hooper [16] shows the effective stream function ϕ_α in each fluid satisfies the equations

$$\begin{aligned} \left(\frac{d^2}{dy^2} - a^2\right)^2 \phi_1(y) = i\alpha Re \left\{ [u_1(y) - c] \left(\frac{d^2}{dy^2} - a^2\right) \right. \\ \left. - u_1''(y) \right\} \phi_1(y), \quad -1 < y < 0, \end{aligned} \tag{6.4}$$

$$\begin{aligned} \left(\frac{d^2}{dy^2} - a^2\right)^2 \phi_2(y) = \frac{i\alpha Re}{m} \left\{ [u_2(y) - c] \left(\frac{d^2}{dy^2} - a^2\right) \right. \\ \left. - u_2''(y) \right\} \phi_2(y), \quad 0 < y < n, \end{aligned} \tag{6.5}$$

where a is the wavenumber and c is the growth rate due to a disturbance of form $\exp[ia(x - ct)]$.

The boundary conditions on the plates are

$$\phi_1(-1) = 0, \quad \phi_1'(-1) = 0, \quad \phi_2(n) = 0, \quad \phi_2'(n) = 0. \tag{6.6}$$

The interface conditions due to continuity of velocity components and continuity of shear and normal stresses are, on $y = 0$,

$$\begin{aligned}\phi_1 &= \phi_2 \quad (= \phi(0)), \\ \phi_1' &= \phi_2' + \frac{\phi(0)}{[c - u_1(0)]} u_1'(0) \left(\frac{1 - m}{m} \right), \\ \phi_1'' + a^2 \phi_1 &= m(\phi_2'' + a^2 \phi_2),\end{aligned}\tag{6.7}$$

$$\begin{aligned}-iaRe([c - u_1(0)]\phi_1' + a_1\phi_1) + iraRe([c - u_1(0)]\phi_2' + a_2\phi_2) \\ - \phi_1''' + 3a^2\phi_1' + m(\phi_2''' - 3a^2\phi_2') = \frac{iaRe}{[c - u_1(0)]} \left(\frac{1}{F^2} + a^2S \right) \phi,\end{aligned}$$

where $r = \rho_1/\rho_2$, F is a non-dimensional form of the density difference $\rho_2 - \rho_1$, and S is a non-dimensional form of the interfacial tension, Yih [29]. Actually, Hooper [16] restricts attention to equal densities and zero interfacial tension, i.e. $r = 1, S = 0$, as we do in computations. However, we wish to indicate that the D^2 method may be applied to the complete boundary condition due to continuity of normal stress, (6.7)₄, derived by Yih [29].

To implement (6.7)₄ in practice we use (6.7)₂ to rewrite it as

$$\begin{aligned}-iaRe([c - u_1(0)]\phi_1' + a_1\phi_1) + iraRe([c - u_1(0)]\phi_2' + a_2\phi_2) \\ - \phi_1''' + 3a^2\phi_1' + m(\phi_2''' - 3a^2\phi_2') = \frac{iamRe}{u_1'(0)(1 - m)} \left(\frac{1}{F^2} + a^2S \right) (\phi_1' - \phi_2'),\end{aligned}\tag{6.8}$$

with $m \neq 1$. A discrete version of (6.8) is easily added to a Chebyshev formulation, following the lines given below.

Henceforth, we restrict attention to Hooper's [16] problem for which $r = 1, S = 0$. To solve (6.4)-(6.7) by a D^2 Chebyshev tau - QZ algorithm technique we first map $y \in (-1, 0)$ and $y \in (0, n)$ to the domains $(-1, 1)$ by the transformations

$$z_1 = -2y - 1, \quad z_2 = \frac{2}{n}y - 1;\tag{6.9}$$

note that $z = -1$ becomes the interface in both cases.

Define now $\phi(z_1) = \phi_1(y), \psi(z_2) = \phi_2(y)$, and then define the differential operators

L_1, L_2 , and functions ξ, ω by

$$\begin{aligned}
L_1\phi &\equiv \left(4\frac{d^2}{dz_1^2} - a^2\right)\phi, \\
L_1\phi &= \xi, \\
L_2\psi &\equiv \left(\frac{4}{n^2}\frac{d^2}{dz_2^2} - a^2\right)\psi, \\
L_2\psi &= \omega,
\end{aligned} \tag{6.10}$$

so we rewrite the differential equations (6.4), (6.5) as

$$\begin{aligned}
L_1\phi - \xi &= 0, \\
L_1\xi - iaReu_1\xi + 2A_1iaRe\phi &= -ciaRe\xi, \\
L_2\psi - \omega &= 0, \\
L_2\omega - i\frac{aRe}{m}u_2\omega + 2A_2i\frac{aRe}{m}\psi &= -ci\frac{aRe}{m}\omega.
\end{aligned} \tag{6.11}$$

The idea is to write

$$\phi = \sum_{n=0}^{N+2} \phi_n T_n(z_1), \quad \xi = \sum_{n=0}^{N+2} \xi_n T_n(z_1), \quad \psi = \sum_{n=0}^{N+2} \psi_n T_n(z_2), \quad \omega = \sum_{n=0}^{N+2} \omega_n T_n(z_2).$$

The boundary conditions (6.6) become

$$\phi(1) = \frac{d\phi}{dz_1}(1) = 0, \quad \psi(1) = \frac{d\psi}{dz_2}(1) = 0. \tag{6.12}$$

The interface boundary conditions are, on $z_1 = z_2 = -1$,

$$\begin{aligned}
\phi - \psi &= 0, \\
\xi + 2a^2\phi - m\omega - 2a^2m\psi &= 0, \\
\frac{d\xi}{dz_1} - 2a^2\frac{d\phi}{dz_1} + \frac{m}{n}\frac{d\omega}{dz_2} - \frac{2m}{n}a^2\frac{d\psi}{dz_2} &= 0,
\end{aligned} \tag{6.13}$$

$$c\left(\frac{d\phi}{dz_1} + \frac{1}{n}\frac{d\psi}{dz_2}\right) = \frac{d\phi}{dz_1} + \frac{1}{n}\frac{d\psi}{dz_2} - \frac{a_1}{2}\left(\frac{1-m}{m}\right)\phi.$$

The Chebyshev tau version of (6.11)-(6.13) yields a $4(N + 3) \times 4(N + 3)$ matrix system like (1.21) where

$$A_r = \begin{pmatrix} 4D^2 - a^2I & -I & 0 & 0 \\ BC1 & 0 \dots 0 & 0 \dots 0 & 0 \dots 0 \\ BC2 & 0 \dots 0 & 0 \dots 0 & 0 \dots 0 \\ 0 & 4D^2 - a^2I & 0 & 0 \\ BC5 & BC5 & BC5 & BC5 \\ BC6 & BC6 & BC6 & BC6 \\ 0 & 0 & \frac{4}{n^2}D^2 - a^2I & 0 \\ 0 \dots 0 & 0 \dots 0 & BC3 & 0 \dots 0 \\ 0 \dots 0 & 0 \dots 0 & BC4 & 0 \dots 0 \\ 0 & 0 & 0 & \frac{4}{n^2}D^2 - a^2I \\ BC7 & BC7 & BC7 & BC7 \\ BC8 & BC8 & BC8 & BC8 \end{pmatrix}$$

$$A_i = \begin{pmatrix} 0 & 0 & 0 & 0 \\ 0 \dots 0 & 0 \dots 0 & 0 \dots 0 & 0 \dots 0 \\ 0 \dots 0 & 0 \dots 0 & 0 \dots 0 & 0 \dots 0 \\ 2aA_1RI & -aRu_1 & 0 & 0 \\ 0 \dots 0 & 0 \dots 0 & 0 \dots 0 & 0 \dots 0 \\ 0 \dots 0 & 0 \dots 0 & 0 \dots 0 & 0 \dots 0 \\ 0 & 0 & 0 & 0 \\ 0 \dots 0 & 0 \dots 0 & 0 \dots 0 & 0 \dots 0 \\ 0 \dots 0 & 0 \dots 0 & 0 \dots 0 & 0 \dots 0 \\ 0 & 0 & 2\frac{A_2aR}{m}I & -\frac{aR}{m}u_2 \\ 0 \dots 0 & 0 \dots 0 & 0 \dots 0 & 0 \dots 0 \\ 0 \dots 0 & 0 \dots 0 & 0 \dots 0 & 0 \dots 0 \end{pmatrix}$$

$$B_r = \begin{pmatrix} 0 & 0 & 0 & 0 \\ 0 \dots 0 & 0 \dots 0 & 0 \dots 0 & 0 \dots 0 \\ 0 \dots 0 & 0 \dots 0 & 0 \dots 0 & 0 \dots 0 \\ 0 & 0 & 0 & 0 \\ 0 \dots 0 & 0 \dots 0 & 0 \dots 0 & 0 \dots 0 \\ 0 \dots 0 & 0 \dots 0 & 0 \dots 0 & 0 \dots 0 \\ 0 & 0 & 0 & 0 \\ 0 \dots 0 & 0 \dots 0 & 0 \dots 0 & 0 \dots 0 \\ 0 \dots 0 & 0 \dots 0 & 0 \dots 0 & 0 \dots 0 \\ 0 & 0 & 0 & 0 \\ 0 \dots 0 & 0 \dots 0 & 0 \dots 0 & 0 \dots 0 \\ BC8 & BC8 & BC8 & BC8 \end{pmatrix}$$

and

$$B_i = \begin{pmatrix} 0 & 0 & 0 & 0 \\ 0 \dots 0 & 0 \dots 0 & 0 \dots 0 & 0 \dots 0 \\ 0 \dots 0 & 0 \dots 0 & 0 \dots 0 & 0 \dots 0 \\ 0 & -aRI & 0 & 0 \\ 0 \dots 0 & 0 \dots 0 & 0 \dots 0 & 0 \dots 0 \\ 0 \dots 0 & 0 \dots 0 & 0 \dots 0 & 0 \dots 0 \\ 0 & 0 & 0 & 0 \\ 0 \dots 0 & 0 \dots 0 & 0 \dots 0 & 0 \dots 0 \\ 0 \dots 0 & 0 \dots 0 & 0 \dots 0 & 0 \dots 0 \\ 0 & 0 & 0 & -\frac{aR}{m}I \\ 0 \dots 0 & 0 \dots 0 & 0 \dots 0 & 0 \dots 0 \\ 0 \dots 0 & 0 \dots 0 & 0 \dots 0 & 0 \dots 0 \end{pmatrix}$$

where u_1 and u_2 are the Chebyshev representations of $u_1(z_1)$, $u_2(z_2)$, and

$$\mathbf{x} = (\phi_0, \dots, \phi_N, \xi_0, \dots, \xi_N, \psi_0, \dots, \psi_N, \omega_0, \dots, \omega_N)^T.$$

Let us assume N is rescaled so that each block is $N \times N$, i.e. each matrix is $4N \times 4N$. The BC1 terms, in row $N - 1$, stand for the Chebyshev version of the boundary conditions $\phi(1) = 0$, and the BC2 terms, in row N , mean the boundary condition $\phi'(1) = 0$; these are written with the aid of the properties $T_n(\pm 1) = (\pm 1)^n$, $T'_n(\pm 1) = (\pm 1)^{n-1}n^2$. Likewise the BC3 and BC4 terms, in rows $3N - 1$ and $3N$, respectively, overwrite with the boundary conditions $\psi(1) = 0$ and $\psi'(1) = 0$. The BC5 - BC8 rows stand for the interface boundary conditions (6.13). The expression BC5 overwrites with

$$\phi(-1) \quad 0 \quad -\psi(-1) \quad 0$$

i.e.

$$1 - 1 \dots 1 - 1 \quad 0 \dots 0 \quad -1 \ 1 \dots -1 \ 1 \quad 0 \dots 0$$

where each group, e.g. $1 - 1 \dots 1 - 1$, etc., contains N terms. The expression BC6 stands for

$$2a^2 \phi(-1) \quad \xi(-1) \quad -2a^2 m \psi(-1) \quad -m\omega(-1)$$

while the notation BC7 overwrites with

$$-2a^2 \frac{d\phi}{dz_1}(-1) \quad \frac{d\xi}{dz_1}(-1) \quad -2\frac{m}{n}a^2 \frac{d\psi}{dz_2}(-1) \quad \frac{m}{n} \frac{d\omega}{dz_2}(-1).$$

The interface boundary condition (6.13)₄ involving c has to be written into row $4N$ of A_r and B_r , via BC8; the part going into A_r is

$$\frac{d\phi}{dz_1}(-1) - \frac{1}{2}a_1 \left(\frac{1-m}{m} \right) \phi(-1) \quad 0 \quad \frac{1}{n} \frac{d\psi}{dz_2}(-1) \quad 0$$

whereas into B_r we write

$$\frac{d\phi}{dz_1}(-1) = 0 \quad \frac{1}{n} \frac{d\psi}{dz_2}(-1) = 0$$

To check the code we ran it with $R = 10^4$, $a = 1$, $m = n = 1$, $u_n = 0$ and we reproduce Orszag's [22] results, cf. section 2, although a "degenerate" interface eigenvalue of $(1,0)$ is found. That this is acceptable follows from boundary condition $(6.13)_4$ where $c = 1$ is a solution.

Employing 150 polynomials in each of ϕ, ξ, ψ and ω we have made several calculations of spectra. Our choice of parameters was guided by Hooper's [16] results for the leading eigenvalue at criticality, i.e. the value of c between linear stability and instability for which $c_i = 0$. Her numerical technique was an orthonormalization type shooting method which locates one eigenvalue. We have not previously seen calculations of the spectra for the superposed fluids problem. Hooper [16] reports that for $m = 2, n = 1.2$ there are two distinct modes of possible instability if the Reynolds number is sufficiently high; one due to shear in the bulk of the fluids whereas the other is due to the interface effect. She reports that the orthonormalization technique could not determine the growth rates of the shear mode to sufficient accuracy. We have seen no trouble with this employing the method outlined here. In figure 7 we include the spectrum obtained for the parameter values $Re = 10^4, u_n = 0, m = 2, n = 1.2, a = 1$, which is well into the shear instability zone of Hooper [16], which she reports begins around $Re = 7400$. The shear mode is the one crossing the $c_i = 0$ axis at the upper left whereas the interface mode is the one in the top right corner. The splitting of the tail is not a numerical instability as we confirmed by calculation with 128 bit arithmetic. This feature is, in fact, observed as m increases from 1. The actual numerical values of the two leading eigenvalues in figure 7 are presented in table 5.

Mode Type	Eigenvalue c
interface	$1.003907431 + 0.1791888368E - 02i$
shear	$0.2578942002 + 0.8778915187E - 03i$

Table 5. Numerical values of the two leading eigenvalues in figure 7.

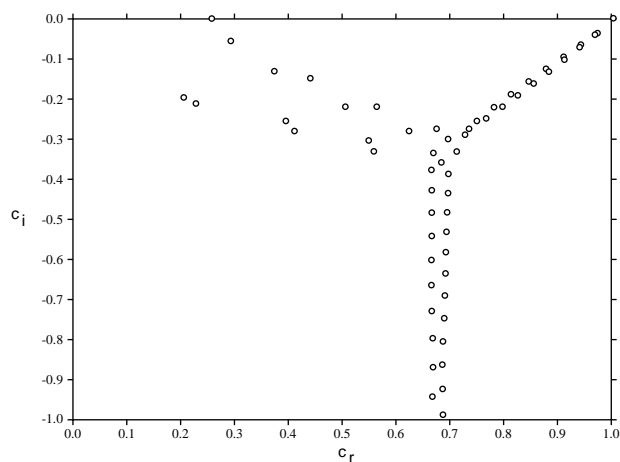


Figure 7

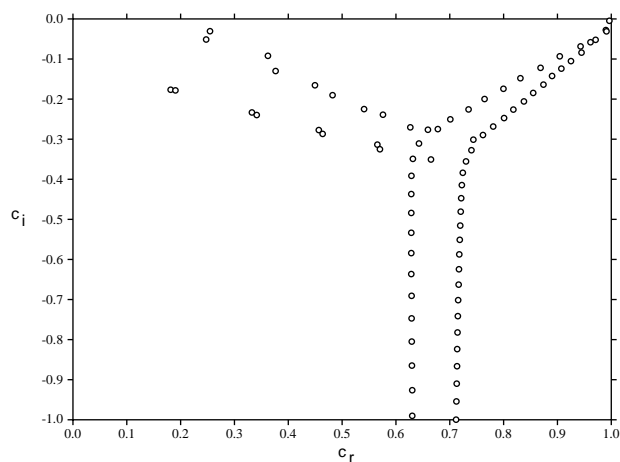


Figure 8

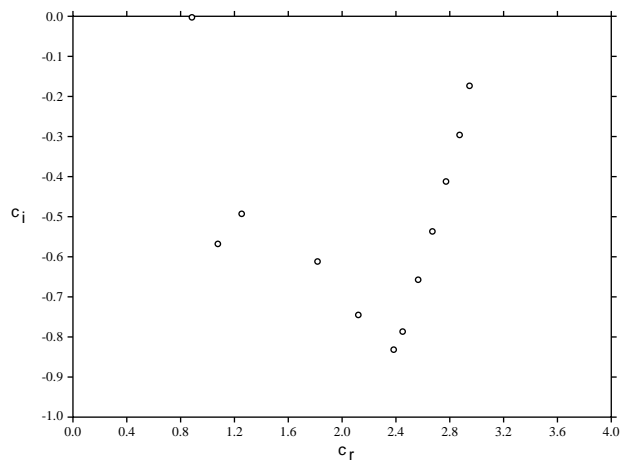


Figure 9

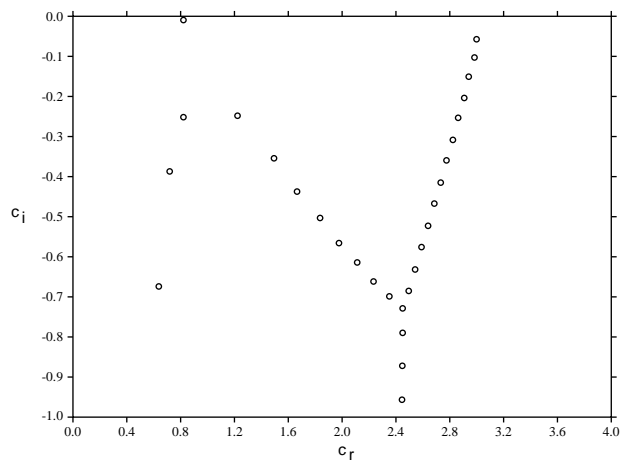


Figure 10

Figure 7 The spectrum for (6.11)-(6.13). $Re = 10^4, a = 1, m = 2, n = 1.2, u_n = 0$.

Figure 8 The spectrum for (6.11)-(6.13). $Re = 10^4, a = 1, m = 2, n = 2, u_n = 0$.

Figure 9 The spectrum for (6.11)-(6.13). $Re = 25, a = 1, m = 2, n = 10, u_n = 3$.

Figure 10 The spectrum for (6.11)-(6.13). $Re = 125, a = 1, m = 2, n = 10, u_n = 3$.

Figure 8 shows how the tail splits more as n increases. Notice how for $n = 2$ the shear mode which is clearly unstable at $n = 1.2$ has dropped substantially into the stable zone. Hooper [16] reports that mode crossing occurs as n increases so the two separate modes which are unstable at $n = 1.2$ bifurcate at some intermediate value of n to form one stable mode when $n = 10$. Our investigations of various cases show the shear mode to be less influential when $n = 10$. For example, calculations with $n = 10, m = 2, u_n = 0, Re = 500$ and $a = 0.37$ and $a = 4.5$ show one unstable mode, consistent with graph 5b of [16]. The $a = 4.5$ spectrum shows evidence of a shear like branch, but the leading eigenvalue of this branch is well into the stable zone.

We have three further mpeg movies which may be viewed by opening the following URL with a web browser

<http://www.epm.ornl.gov/~walker/eigenproblems.html>

These contain the parameter evolution of the spectrum of the Hooper [16] problem. The parametric studies are (a) $Re = 200, a = 2, m = 2, u_n = 0$, with n going from 1.2 to 10 in steps of 0.1, which corresponds to a change from Hooper's [16] figure 5a to figure 5b; (b) $a = 1, u_n = 3, m = 2, n = 10$, with Re going from 25 to 125 in steps of 1, which corresponds to figure 6b of [16]; (c) $Re = 100, u_n = 2, m = 2, n = 10$, with a going from 0.3 to 2.3 in steps of 0.02, this corresponding to figure 6a of [16].

The “evolutionary” behaviour is revealing. In the (b) case we see only one leading mode which begins in the stable zone then becomes unstable before again returning to the stable zone, entirely consistent with the neutral curve of [16]. The eigenvalues “emanate” from two points on the $c_i = -1$ axis, one point just below $c_r = 1$ whereas the other is at approximately $c_r = 2.45$. The spectra for the extreme cases $Re = 25$ and $Re = 125$ are shown in figures 9 and 10.

The track in the wave number a , case (c), again shows one leading eigenvalue which begins in the stable region, goes unstable, then stable, and finally unstable, which again is consistent with the neutral curve in [16]. Again, the eigenvalues emanate from two places on the $c_i = -1$ axis, one of these being $c_r \approx 2.1$ while the other varies between $c_r \approx 0.8$ and $c_r \approx 0.6$. The cases $a = 0.3$ and $a = 2.3$ are displayed in figures 11 and 12.

Variation in n in the movie for case (a) is interesting. The leading eigenvalue begins unstable and finishes stable as n is varied from 1.2 to 10, consistent with the neutral curves of [16]. However, at $n \approx 2.9$ this eigenvalue moves sharply down into the stable region while an eigenvalue below moves sharply upward. To the resolution we have they appear to almost “bounce” off each other with the leading eigenvalue then going close to the $c_i = 0$ axis but remaining stable. (Closer examination reveals the eigenvalues do not, in fact, overlap.) In this case the eigenvalues appear to emanate from only one point on

the $c_i = -1$ axis. For n between 1.2 and 2.3 they come from $c_r \approx 0.67$ and at $n \approx 2.9$ this position of emanation begins to move rapidly to the right. Figure 13 displays the spectrum for $n = 10$. Those eigenvalues on the left side are left from the ones which came from below before $n \approx 2.7$. There is definite evidence of some transition at $n \approx 2.9$, where several eigenvalues appear to “bounce” off each other. The two new branches coming from the main right branch begin to form at $n \approx 3.6$. Hooper’s [16] comments on a transition as n increases are consistent with what we have observed.

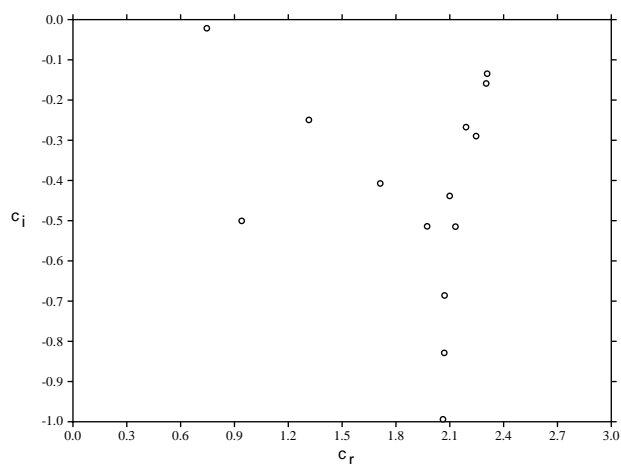


Figure 11

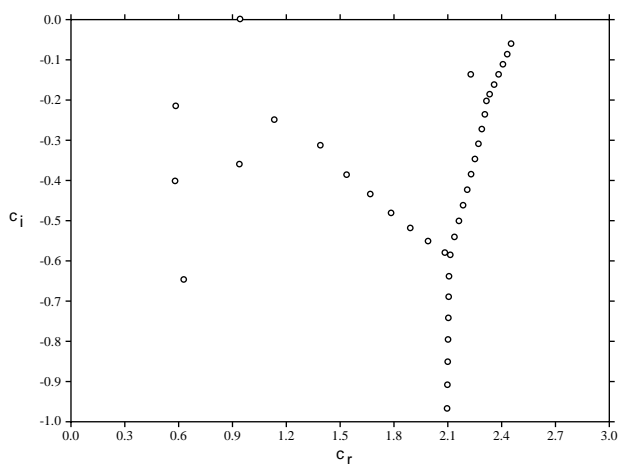


Figure 12

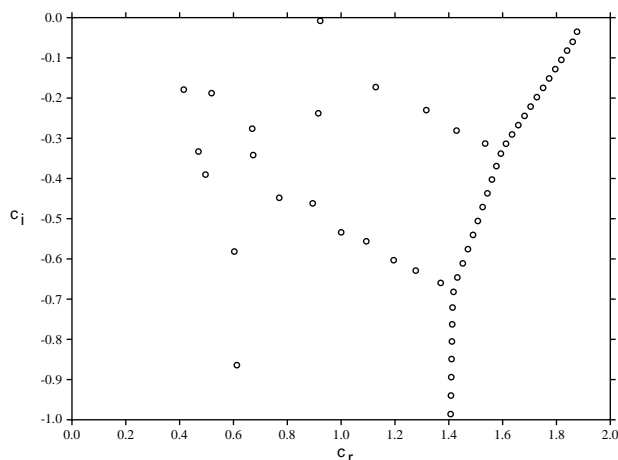


Figure 13

Figure 11 The spectrum for (6.11)-(6.13). $Re = 100, a = 0.3, m = 2, n = 10, u_n = 2$.

Figure 12 The spectrum for (6.11)-(6.13). $Re = 100, a = 2.3, m = 2, n = 10, u_n = 2$.

Figure 13 The spectrum for (6.11)-(6.13). $Re = 200, a = 2, m = 2, n = 10, u_n = 0$.

7. Concluding remarks.

1. As hydrodynamic stability problems become more complex due to incorporation of technologically important effects, the orders of the differential equations involved increase rapidly. Furthermore, there is increasing necessity to calculate a large part of the spectrum. A very important feature of the D^2 Chebyshev tau - QZ algorithm method is that extends

to arbitrarily large systems which may be found, for example, in multi-component convection when many constituents are present and even chemical reactions are taking place, or in such a problem as thermal convection with Hall and ion slip currents simultaneously in effect. The latter problem is twelfth order even without flow effects. In this case very large systems of algebraic equations are encountered especially when the differential equations are stiff, or higher dimensions are considered, as in the plane Poiseuille or Couette flow problems coupled with effects such as multi-component diffusion and thermal convection, or Hall and ion slip MHD influences; such problems have a wide practical application, see e.g. Mulone [21]. For such classes of problem we see that the precision representation of a real number presents a difficulty. The D method of Lindsay & Ogden [18] would appear in some ways desirable because of the $O(M)$ growth of coefficients; however, the fact that the matrices are each of size $JM \times JM$ where J is the order of the system is a very severe restriction. To give an explicit example, the problem of thermal convection with two competing species as studied in [28] if coupled with Couette and / or Poiseuille flow, Hall and ion slip effects, in the case of one fluid overlying another would give rise to two 16th order systems and the resulting matrices in the D method would be $32M \times 32M$; if we require 200 polynomials for accurate resolution this means finding the eigenvalues of a 6400×6400 generalised matrix problem. Even a D^2 method for a large number of polynomials and extended precision calculation requires a large amount of memory and a long run time; the problem alluded to above would require 3200×3200 matrices for 200 polynomials. The very large matrix systems which will be encountered in stability studies on practical problems like that quoted above are precisely the domain for application of parallel software libraries, such as ScaLAPACK Choi *et al.* [6], Dongarra & Walker [10]. Unfortunately, however, at the time of writing a parallel version of the QZ algorithm is not yet available in the ScaLAPACK library. Another line of attack is to use the Arnoldi (iterative) method, see [6], and this will form part of future work.

2. As a further check on accuracy, we computed the sensitivities, Stewart & Sun [25], defined as

$$s^{(i)} = \frac{\|\mathbf{x}_i\| \|\mathbf{y}_i\|}{\mathbf{x}_i^H \mathbf{y}_i} \quad (7.1)$$

for the problem (1.1) with A and B defined as in this section; here \mathbf{x} and \mathbf{y} are right and left eigenvectors of (1.1), respectively. The quantity $\log_{10} s^{(i)}$ is a measure of the number of digits one loses in accuracy. We also considered using the chordal metric which leads to sensitivities defined as

$$s^{(i)} = \frac{\|\mathbf{x}_i\| \|\mathbf{y}_i\|}{\sqrt{|\mathbf{y}_i^H A \mathbf{x}_i|^2 + |\mathbf{y}_i^H B \mathbf{x}_i|^2}} \quad (7.2)$$

which is a more unitary invariant measure than that given in (7.1). However, it is not clear which sensitivity measure is best since when $B = I$ the generalized eigenvalue problem reduces to the standard case, but the sensitivity given in (7.2) does not reduce to the standard sensitivity. Given that the most appropriate definition of sensitivity is open to debate, we believe that the sensitivity defined by (7.1) is adequate for our purposes, and use this definition in table 7 below which gives the absolute values for the first ten “eigenvalues.” Note that the first three values computed are spurious eigenvalues. By examining $\log_{10}s^{(i)}$ in table 7 it is seen that even in full precision (64 bit arithmetic) high accuracy is expected. The sensitivities for the three spurious eigenvalues are also of the same order as those appropriate to eigenvalues of the physical problem, which indicates that the spurious eigenvalues arise from the discretization, not the QZ algorithm.

Mode Number	Sensitivity	c_r	c_i
1	.104875E+05	.9306062397E-01	.5398774786E+05
2	.955170E+04	-.3477822923E+05	.6583840773E+04
3	.955169E+04	.3477831961E+05	.6583707360E+04
4	.192577E+05	.1008716826E+01	.8889416072E-03
5	.133748E+03	.6644993935E+00	-.1242776632E+00
6	.462979E+03	.7467618987E+00	-.1793830027E+00
7	.113398E+04	.7446257506E+00	-.2683049316E+00
8	.160433E+04	.7127003503E+00	-.3747130589E+00
9	.965561E+03	.6933402508E+00	-.5181828296E+00
10	.140640E+04	.6865584144E+00	-.7191848687E+00

Table 6. The sensitivities of the first ten computed “eigenvalues”. $Re = 100, a = 2, m = 2, n = 1.2, u_n = 0, M = 150$.

3. Future work will investigate the implementation of a parallel version of the QZ algorithm, and the use of the Arnoldi method for solving the generalised eigenproblem. In addition, we intend to examine the regular and singular structure of $A - \lambda B$, to see if this has any bearing on the identification of spurious eigenvalues. This may be done by reducing $A - \lambda B$ to the GUPTRI form of Demmel and Kagström [8,9].

Acknowledgments. This research was supported in part by an appointment to the post-

graduate research program at the Oak Ridge National Laboratory (ORNL) administered by the Oak Ridge Institute for Science and Education. We are very grateful to three anonymous referees for their careful reading of the paper and trenchant suggestions for improvement.

References

1. Abdullah, A.A. & Lindsay, K.A. Some remarks on the computation of the eigenvalues of linear systems. *Math. Models and Methods in Applied Sciences* **1** (1991), 153–165.
2. Anderson, E., Bai, Z., Bischof, C., Demmel, J., Dongarra, J.J., Du Croz, J., Greenbaum, A., Hammarling, S., McKenney, A., Ostrouchov, S. & Sorensen, D. *LAPACK Users' guide* (2nd Edition), SIAM (1995).
3. Butler, K.M. & Farrell, B.F. Three-dimensional optimal perturbations in viscous shear flow. *Phys. Fluids A* **4** (1992), 1637–1650.
4. Canuto, C., Hussaini, M.Y., Quarteroni, A. & Zang, T.A. 1988. *Spectral methods in fluid dynamics*. Springer - Verlag, Berlin - Heidelberg.
5. Chen, K.P. & Crighton, D.G. Instability of the large Reynolds number flow of a Newtonian fluid over a viscoelastic fluid. *Phys. Fluids A* **6** (1994), 152–163.
6. Choi, J., Dongarra, J.J., Pozo, R., Sorensen, D.C. & Walker, D.W. CRPC research into linear algebra software for high performance computers. *Int. J. Supercomputer Applications* **8** (1994), 99–118.
7. Davey, A. A simple numerical method for solving Orr-Sommerfeld problems. *Q. Jl. Mech. Appl. Math.* **26** (1973), 401–411.
8. Demmel, J. & Kaström, B. The Generalized Schur Decomposition of an Arbitrary Pencil $A - \lambda B$: Robust Software with Error Bounds and Applications. Part I: Theory and Algorithms. *ACM Trans. Math. Software* **19** (1993), 160–174.
9. Demmel, J. & Kaström, B. The Generalized Schur Decomposition of an Arbitrary Pencil $A - \lambda B$: Robust Software with Error Bounds and Applications. Part II: Software and Applications. *ACM Trans. Math. Software* **19** (1993), 175–201.
10. Dongarra, J.J. & Walker, D.W. Software libraries for linear algebra computations on high performance computers. *SIAM Review*, **37** (1995), 151–180.

11. Drazin, P.G. & Reid, W.H. *Hydrodynamic stability*. Cambridge University Press (1981).
12. Fearn, D.R. Eigensolutions of boundary value problems using inverse iteration. *J. Comp. Appl. Math.* **34** (1991), 201–209.
13. Fox, L. Chebyshev methods for ordinary differential equations. *The Computer J.* **4** (1962), 318–331.
14. Gardner, D.R., Trogdon, S.A. & Douglas, R.W. A modified tau spectral method that eliminates spurious eigenvalues. *J. Computational Physics* **80** (1989), 137–167.
15. Haidvogel, D.B. & Zang, T. The accurate solution of Poisson's equation by expansion in Chebyshev polynomials. *J. Computational Phys.* **30** (1979), 167–180.
16. Hooper, A.P. The stability of two superposed viscous fluids in a channel. *Phys. Fluids A* **1** (1989), 1133–1142.
17. Huang, W. & Sloan, D.M. The pseudospectral method for solving differential eigenvalue problems. *J. Computational Phys.* **111** (1994), 399–409.
18. Lindsay, K.A. & Ogden, R.R. A practical implementation of spectral methods resistant to the generation of spurious eigenvalues. *Int. J. Numer. Methods Fluids* **15** (1992), 1277–1294.
19. McFadden, G.B., Murray, B.T. & Boisvert, R.F. Elimination of spurious eigenvalues in the Chebyshev tau spectral method. *J. Computational Physics* **91** (1990), 228–239.
20. Moler, C.B. & Stewart, G.W. An algorithm for generalized matrix eigenproblems. *SIAM. J. Numerical Anal.* **10** (1973), 241–256.
21. Mulone, G. On the nonlinear stability of a fluid layer of a mixture heated and salted from below. *Continuum Mech. Thermodyn.* **6** (1994), 161–184.
22. Orszag, S.A. Accurate solution of the Orr - Sommerfeld stability equation. *J. Fluid Mech.* **50** (1971), 689–703.
23. Reddy, S.C. & Henningson, D.S. Energy growth in viscous channel flows. *J. Fluid Mech.* **252** (1993), 209–238.
24. Renardy, Y. Weakly nonlinear behaviour of periodic disturbances in two-layer Couette-Poiseuille flow. *Phys. Fluids A* **1** (1989), 1666–1676.
25. Stewart, G.W. & Sun, J.-G. *Matrix Perturbation Theory*, Academic Press, New York

(1990).

26. Straughan, B. & Walker, D.W. Anisotropic porous penetrative convection. *Proc. Roy. Soc. London A*, **452** (1996), 97–115.
27. Straughan, B. & Walker, D.W. Two very accurate and efficient methods for computing eigenvalues and eigenfunctions in porous convection problems. *J. Computational Phys.* To appear.
28. Straughan, B. & Walker, D.W. Multi-component diffusion and penetrative convection. To appear.
29. Yih, C.S. Instability due to viscosity stratification. *J. Fluid Mech.* **27** (1967), 337–352.
30. Zebib, A. Removal of spurious modes encountered in solving stability problems by spectral methods. *J. Computational Phys.* **70** (1987), 521–525.